

# We are IntechOpen, the world's leading publisher of Open Access books Built by scientists, for scientists

6,900

Open access books available

186,000

International authors and editors

200M

Downloads

Our authors are among the

154

Countries delivered to

TOP 1%

most cited scientists

12.2%

Contributors from top 500 universities



WEB OF SCIENCE™

Selection of our books indexed in the Book Citation Index  
in Web of Science™ Core Collection (BKCI)

Interested in publishing with us?  
Contact [book.department@intechopen.com](mailto:book.department@intechopen.com)

Numbers displayed above are based on latest data collected.  
For more information visit [www.intechopen.com](http://www.intechopen.com)



# Biological Response of Osteoblasts and Osteoprogenitors to Orthopaedic Wear Debris

Richard Chiu and Stuart B. Goodman

*Stanford University Medical School, Department of Orthopaedic Surgery,  
USA*

## 1. Introduction

Total joint replacements are one of the most commonly performed orthopaedic procedures worldwide, with over 700,000 surgeries performed annually in the US to treat arthritic conditions of the hip and knee. One of the major complications of total joint replacement is implant wear and osteolysis, a process that involves continuous shedding of micron- and submicron-sized particles from implant components. Implant particles elicit cascades of inflammatory, osteolytic, and granulomatous reactions from macrophages, osteoclasts, and fibroblasts, causing the prosthesis to become unstable. Since the mid 1990s, *in vitro* studies have shown that wear debris particles inhibit the osteogenic function of osteoblasts and osteoprogenitor cells of human and rodent species. Osteolysis and implant loosening involve not only increased bone resorption by osteoclasts and inflammatory cells, but also reduced bone formation by osteoblasts and their progenitors. This disruption of proliferation, differentiation, function, and survival of osteoblasts prevents the implant from properly integrating with surrounding bone.

The inhibitory effects of implant wear debris on osteoblasts and osteoprogenitors have been demonstrated using particles of metallic (titanium, cobalt chrome), polymeric (polyethylene, PMMA), and ceramic (alumina, zirconia) implants. Human and rodent primary osteoblasts and osteoblast cell lines, such as MG-63 cells, treated with titanium and polyethylene particles in culture, uniformly show reduced type I collagen synthesis with evidence of particle phagocytosis and morphological changes consistent with cell injury and cytoskeletal disorganization on microscopy. Selected studies also show that particles impair osteoblast viability, proliferation, adhesion, extracellular matrix production, and osteogenic protein expression (e.g., alkaline phosphatase). Implant particles uniformly stimulate expression of NF- $\kappa$ B and IL-6, IL-8, PGE<sub>2</sub>, RANKL, M-CSF, and MCP-1, pro-inflammatory factors known to recruit monocyte-macrophages or induce osteoclast differentiation and activity. These studies also indicate that the effect of particles on osteoblasts depends on particle size and composition and the maturational state of the cell. Metal implants such as cobalt chromium and titanium alloys pose an additional risk of metal ion toxicity.

Wear debris particles also inhibit the osteogenic activity of osteoprogenitors and marrow stromal cells (MSCs). Human bone marrow-derived MSCs exposed to titanium particles exhibit reduced proliferation, type I collagen expression, viability, and matrix mineralization with evidence of particle phagocytosis and structural and biochemical changes indicative of

apoptosis. The exposure of human MSCs to BMP-6, FGF-2, IGF-1, and TGF- $\beta$ 1, factors with trophic, osteogenic, and prosurvival effects, partly mitigates the inhibitory effects of titanium particles. Studies have shown that PMMA particles inhibit the osteogenic differentiation of mouse and human bone marrow-derived MSCs and murine MC3T3-E1 pre-osteoblasts. When exposed to PMMA particles, these cells show a dose-dependent decrease in proliferation, alkaline phosphatase expression, and matrix mineralization. MC3T3-E1 cells also show reduced viability and expression of osteogenic transcription factors Runx2, osterix, and Dlx5, and changes in expression patterns of MAP kinase signaling molecules. Treating MC3T3-E1 cells with OP-1 (BMP-7) partly mitigates the inhibitory effect of PMMA particles. Polyethylene particles (ultrahigh molecular weight) also inhibit the osteogenic differentiation of mouse MSCs and MC3T3-E1 cells in a similar fashion. Phagocytosis of implant particles by MSCs and osteoprogenitors mediates the inhibitory effects and causes morphological changes indicative of cell damage.

Biological responses of osteoblasts and osteoprogenitors to orthopaedic wear debris have been studied in vitro and in vivo. In vitro studies have used osteoblast cell lines or primary osteoblasts isolated from human trabecular bone or rat calvarium, and MSCs and osteoprogenitors derived from bone marrow of human or mouse femur and tibia. Orthopaedic particles are obtained from commercial sources or extracted from membrane tissues or synovial fluids of failed hip or knee replacements or serum of in vitro wear simulator tests. In vivo tissue responses to wear debris particles have been studied with the femoral intramedullary injection model or the bone harvest and drug test chambers. Clinically, the inhibition of osteoblast function and differentiation by implant wear debris reduces bone formation in the prosthetic bed and predisposes the implant toward accelerated osteolysis. The inhibitory effects of wear particles appear to be partly mitigated by growth factors with trophic and osteogenic effects. Prevention strategies and therapies for osteolysis and implant loosening will involve development of wear-resistant biomaterials and pharmacological modalities for increasing bone formation in the implant.

## 2. Total joint arthroplasty

Total joint arthroplasty is the surgical replacement of a diseased, dysfunctional joint with a prosthetic joint. In the United States alone, over 400,000 total knee and 300,000 total hip replacements are performed annually to treat joint diseases such as osteoarthritis, rheumatoid arthritis, osteonecrosis, and arthritic conditions caused by autoimmunity, trauma, crystal deposits, or hip dysplasia. In arthritis, the layer of articular cartilage in the joint is worn away by the disease process, exposing the underlying bone to friction and causing the joint to become inflamed, painful, and stiff. When conservative measures such as anti-inflammatory drugs, corticosteroids, physical therapy, and joint preserving procedures fail to relieve pain and restore function, joint replacement is considered the next line of treatment. The procedure effectively alleviates pain and restores joint function, and is associated with an implant survival rate of at least 90% at 10 years. Elderly and middle-aged persons constitute the great majority of patients and are considered better candidates than younger persons given that lower physical activity prolongs the longevity of the implant. Since the introduction of the modern arthroplasty in the 1960s, the procedure has benefited millions of patients in the United States and worldwide.

The modern arthroplasty is a modular system composed of separable components. This modularity allows the surgeon to tailor the prosthesis to match the patient's requirements,

or to replace components without removing the entire implant when the need for revision surgery arises. The current orthopaedic market offers a large range of prosthetic components based on different surgeon preferences for implant materials, designs, wear properties, and fixation techniques, and considerations for patient age, anatomy, bone stock, and activity level. The modern arthroplasty is based on a prototypical design in which two metal units articulate with an intervening cushion that is a plastic spacer that serves as a low-friction surface. Using total hip arthroplasty as an example, the prosthesis generally consists of four components: a round, highly polished femoral head made of cobalt chromium alloy that articulates with a concave acetabular liner made of ultrahigh molecular weight polyethylene in a "ball and socket" fashion; a femoral stem made of cobalt chromium or titanium alloy inserted into the medullary canal of the femur; and a dome-shaped acetabular shell made also of cobalt chromium or titanium alloy that provides a platform for fixing the acetabular liner to the acetabulum via screws, pegs, and roughened, coated, or porous surfaces. The sizes and diameters of the modular components are chosen such that the acetabular liner fits precisely in the acetabular shell and the femoral head in the concavity of the acetabular liner. Implant materials must withstand cyclic forces and not fail under load, meaning they must have appropriately high tensile, compressive, yield, shear, and fatigue strengths.

Metals commonly used in joint implants include pure titanium, titanium alloy with 6% aluminium and 4% vanadium (Ti-6Al-4V), and cobalt alloy with 27-30% chromium and 5-7% molybdenum (Co-Cr-Mo). These metals are chosen based on their light weight, biocompatibility (lack of reaction to body fluids and tissues), corrosion resistance, and ability to integrate with adjacent bone. Cobalt chromium alloy is additionally characterized by high tensile strength, toughness, and resistance to wear, fatigue, and fracture, which makes it a highly suitable material for articulating surfaces. The incorporation of molybdenum into the cobalt chromium alloy increases its strength and corrosion resistance. Titanium metals are relatively light (density 4.5 g/cm<sup>3</sup>) and are also corrosion resistant due to a protective oxide layer (TiO<sub>2</sub>) that forms on its surface. However, because of their lower shear strength, surface hardness, and wear resistance than cobalt chromium alloys, titanium metals are used mainly for the femoral stem and acetabular shell, while cobalt chromium is used for the femoral head. Stainless steel grades 316 and 316L are also used in joint replacements, but mainly as screws, plates, and rods for implant fixation due to their greater tendency to corrode and leach toxic substances than cobalt chromium or titanium alloys. Cobalt chromium alloy and titanium metals have served as successful femoral implants since their introduction in the 1960s. Newer alloys are currently available and hope to improve on the properties of conventional alloys. Issues exist however, regarding wear debris production, which is the focus of this chapter.

Ultrahigh molecular weight polyethylene (UHMWPE) is the main polymer used in joint implants (Kurtz, 2004). Polyethylene molecules of this molecular weight range are 3 to 6 million daltons, approximately 10 times that of conventional polyethylene molecules. UHMWPE solid is characterized by low friction, biocompatibility, and high toughness, impact and tensile strength, and wear resistance. Because of these qualities, UHMWPE is used as the articulating material in almost all joint prostheses, including those of the shoulder, elbow, and ankle. UHMWPE derives its strength from its large molecules which exert a vast degree of van der Waals forces between its linearly aligned molecules. In addition, the large size of UHMWPE molecules causes less efficient packing, which yields lower density and crystallinity. These properties are also beneficial to its clinical

performance since lower density decreases weight, and lower crystallinity increases resistance to cracks and wear. The strength and wear properties of UHMWPE are also affected by cross-linking between molecules, with greater cross-linking improving strength, toughness, and wear resistance. This has led to the development of highly cross-linked UHMWPE, which consists of highly branched polyethylene molecules. Cross-linking between the branched molecules is induced by irradiation of the material at high gamma doses (50,000 to 150,000 Gy), often followed by annealing. Different cross-linking protocols exist, resulting in variance in mechanical properties. Wear experiments have shown that cross-linked material has significantly lower wear rates compared to conventional UHMWPE; however clinical studies are needed to evaluate its performance in patients in the long term. Ten year wear rates have been extremely encouraging. Conventional UHMWPE has served as an excellent load-bearing material in the past four decades. Despite its excellent wear properties, however, it continues to be the main source of wear debris particles that elicit chronic inflammation and osteolysis.

Polymethylmethacrylate (PMMA) bone cement is used as a grout for fixing prosthetic components such as the femoral stem or acetabular shell to adjacent bone. Prostheses can be anchored to bone by cementless or cemented techniques. Although the choice of cementless versus cemented fixation is dependent on the surgeon, cementless fixation is generally preferred for younger patients with good bone stock, while cemented fixation is preferred by some older patients with poor bone stock. Cementless prostheses employ roughened or porous surfaces for long-term bone ingrowth and implant stability. The porous coating in a femoral stem, for instance, may extend over the entire length of the implant or only over the metaphyseal and proximal diaphyseal areas. Bone ingrowth into porous coatings takes place over weeks or months to achieve fixation. In cemented arthroplasties, powder is mixed with a monomer solution to form a polymer. The cement fills spaces between implant and bone and then solidifies in an exothermic process. Bone cement is most commonly applied to the femoral stem to achieve fixation with surrounding bone. PMMA is usually mixed with radiopacifiers such as barium sulfate to make it visible on radiograph, and sometimes with antibiotics to prevent infection. Although highly successful as a grouting agent, PMMA has good compressive strength but relatively poor fatigue and shear strength under load. PMMA may also leach monomers and cause surrounding thermal necrosis that can induce formation of fibrous tissue layer at the bone implant interface.

Ceramic materials, alumina (aluminum oxide  $\text{Al}_2\text{O}_3$ ) and zirconia (zirconium oxide  $\text{ZrO}_2$ ), have been used as alternatives to metal alloys and polyethylene for weight-bearing surfaces because of their high wear resistance, low friction, hardness, and biocompatibility. Interest in ceramics has arisen from the issue of wear debris production from conventional metal-on-polyethylene surfaces and the search for better wear-resistant materials. Experiments have shown that ceramics outperform metals and polyethylene in this respect. Ceramic-on-ceramic articulations show significantly lower coefficients of friction and wear rates than conventional metal-on-polyethylene articulations. Ceramic wear debris particles are also reported to be less bioreactive and inflammatory than metal or polyethylene debris. Despite their low wear and friction, ceramics are brittle and prone to fracture or cracking. For this reason, ceramic implants are considered mainly for younger patients because they benefit more from the reduced rates of wear debris production. Alumina is now the main ceramic available in the orthopaedic market. Alternative bearing combinations reported to have lower wear rates are ceramic-on-polyethylene and metal-on-metal articulations, though the

long-term clinical performance of these implants need to be assessed, particularly with respect to wear, osteolysis, metal ion toxicity, and adverse tissue reactions.

The modern total knee arthroplasty is modular and consists of distal femoral and proximal tibial components made of cobalt chromium or titanium alloy, and a UHMWPE tibial insert in between that articulates with the femoral component. The distal femoral component is round-ended resembling the shape of the femoral condyles; the proximal tibial component has a flat top which holds the UHMWPE tibial insert, and a stemmed bottom for insertion in the tibial medullary cavity. Like hip arthroplasties, knee implants can be cementless or cemented, the choice of which is surgeon-dependent, and older patients > 70 years of age have longer implant survival than young patients due to lower physical activity. Cementless knee implants contain porous coatings that allow bone ingrowth. However, unlike hip arthroplasties, cementless knee implants are less desirable than cemented ones due to the higher incidence of tibial loosening and polyethylene wear. Total shoulder arthroplasties are designed much like the hip prosthesis: they consist of modular units and are based on a humeral stem that articulates with a glenoid implant in a "hemisphere-socket" fashion. The shoulder prosthesis can also take form of a normal or reverse shoulder design. In the normal shoulder design, the humeral stem is connected to convex humeral head, which articulates with a concave glenoid implant. In the reverse shoulder design, the humeral stem is connected to a humeral neck with a concave surface that articulates with a convex "glenoid sphere," which in turn is linked to a glenoid fixation implant. In both designs, a low-friction UHMWPE insert is cushioned between the articulating "concave-convex" units, similar to the hip and knee prostheses. The humeral stem and neck and glenoid fixation devices are made of cobalt chromium or titanium metal, while the highly polished humeral head and glenoid sphere are made of cobalt chromium. The glenoid fixation device is attached to glenoid cavity with compression screws. Like hip and knee prostheses, shoulder implants can be cementless or cemented. Cementless shoulder implants have porous coatings for bone ingrowth or holes for screw fixation. Cement may be applied to humeral and glenoid implants when bone is fragile. Arthroplasties of other joints such as the elbow and ankle employ the same design of two metal components articulating on a UHMWPE insert.

Clinical complications that are common to all total joint arthroplasties include implant fracture, infection, dislocation, nerve palsy, vascular injury, thromboembolism, and most importantly, *osteolysis and aseptic loosening* caused by biological reactions to *particulate debris* produced from *implant wear*. The rest of this chapter will be devoted to issues concerning wear, osteolysis, and implant loosening, which are the most common and important reason arthroplasties are brought in for revision surgery. Currently, 10% of all total hip and knee replacements succumb to this complication at 10 years. Revision arthroplasties are much more difficult to perform and have a substantially lower implant survival rate than the primary arthroplasty.

### 3. Implant wear and osteolysis

One of the most significant clinical complications of total joint arthroplasty is implant loosening and osteolysis associated with wear debris (Wright & Goodman, 2001). This scenario accounts for the majority of revision surgeries performed for failed hip and knee implants. Approximately 80,000 revision surgeries are performed annually in the United States for loosening and osteolysis of the hip and knee. Symptoms associated with osteolysis such as pain and decreasing function usually do not appear until the lesion is fairly

advanced radiographically. Revision surgery is aimed at replacing loose implant units, removing diseased tissues and debris particles, repairing bone defects caused by osteolysis, thus relieving pain and restoring function. Revision surgeries are more costly, harder to perform, and less successful than the primary surgery.

Osteolysis is caused by particulate debris generated from wear between implant components, particularly by those of load-bearing, articulating surfaces such as the UHMWPE acetabular liner and cobalt chromium femoral head of a hip prosthesis, or the tibial UHMWPE insert and cobalt chromium femoral components of a knee prosthesis. Wear at these articulating surfaces can produce up to hundreds of millions of submicron particles each year. Wear particles migrate through interfaces between implant, cement, and bone, screw holes, or crevices in these materials to enter surrounding tissue. Osteolysis of the hip, for instance, occurs in the acetabulum behind the acetabular shell where wear particles can access peri-implant tissues through screw holes or interfaces of the polyethylene liner, and along the endosteal margins of the femoral medullary canal directly exposed to particles. Wear debris is also produced from non-articulating surfaces, such as backside wear between UHMWPE insert and acetabular shell or tibial tray, micro-movements at sheared or fractured cement interfaces with implant or bone, or friction around loosened metallic stems or screws. Wear is also accelerated by corrosion, oxidation, or fracture.

The main source of wear debris particles is the UHMWPE insert or liner at the surface of articulation. Although UHMWPE has low friction, high wear resistance, and good impact strength, conventional polyethylene wears at an average linear rate of 0.1-0.2 mm/year, or volumetric wear rate of 50-100 mm<sup>3</sup>/year, against cobalt chromium femoral heads. The great majority of UHMWPE wear debris is submicron-sized, more than 90% of which are less than 1.0 μm in diameter, the mean being 0.5 μm. Ceramic particles are also on the order of 0.5-0.7 μm in diameter. Cobalt chromium and titanium metal wear debris are mostly on the nanometer scale, averaging 50 nm in size, roughly 1/10 the average size of polyethylene debris. Volumetric wear rate of metals is an order of magnitude lower than that UHMWPE, but because the particles are also much smaller in size, the number of particles produced is still significantly greater than that of polyethylene. New bearing surfaces such as highly crosslinked polyethylene, metal-on-metal (cobalt chromium), and ceramic-on-ceramic (alumina), have substantially reduced wear rates as shown by simulator tests and implant retrievals. However, particulate debris of the same size, whether it is polymeric or ceramic, and in most cases of metallic debris, elicits similar biological reactions. The concentration of particles appears to be the strongest factor dictating the degree of inflammation.

Wear debris particles infiltrate surrounding tissue and elicit a cascade of biologic events involving pro-inflammatory factor secretion, fibrous membrane formation, and bone resorption, processes that may culminate in loosening of the prosthesis. These events are mediated by macrophages, osteoclasts, fibroblasts, osteoblasts, and their progenitors (Tuan et al., 2008). The majority of wear particles are submicron to nanometer in size, and the size range of particles capable of activating and being phagocytosed by these cells is about 0.3 to 10 μm. Macrophages resident in peri-prosthetic tissue, also called histiocytes, are the primary cells to react to particles. These cells phagocytose particles and release a multitude of pro-inflammatory cytokines, chemokines, arachidonic acid metabolites, and degradative enzymes. The major cytokines that mediate inflammation and bone destruction are TNF-α, IL-1α, and IL-1β, but others that directly or indirectly increase bone resorption are IL-6, IL-8,

PGE<sub>2</sub>, RANKL, M-CSF, GM-CSF, and MCP-1. These cytokines recruit distant inflammatory cells such as neutrophils and monocytes (via IL-8 and MCP-1 respectively), directly stimulate osteoclasts to resorb bone (via IL-6, RANKL, M-CSF), induce the activity of macrophages (via IL-1, GM-CSF, M-CSF), kill bone forming cells (via TNF- $\alpha$ ), participate in matrix degradation (via MMP-2, MMP-9), or induce other cells such as osteoblasts to release RANKL, MMPs, collagenases (via IL-1, TNF- $\alpha$ ). Macrophage release of proinflammatory factors after particle phagocytosis is mediated by transcription factor NF- $\kappa$ B, which is activated by the upstream MAPK (mitogen-activated protein kinase) pathway. Studies have

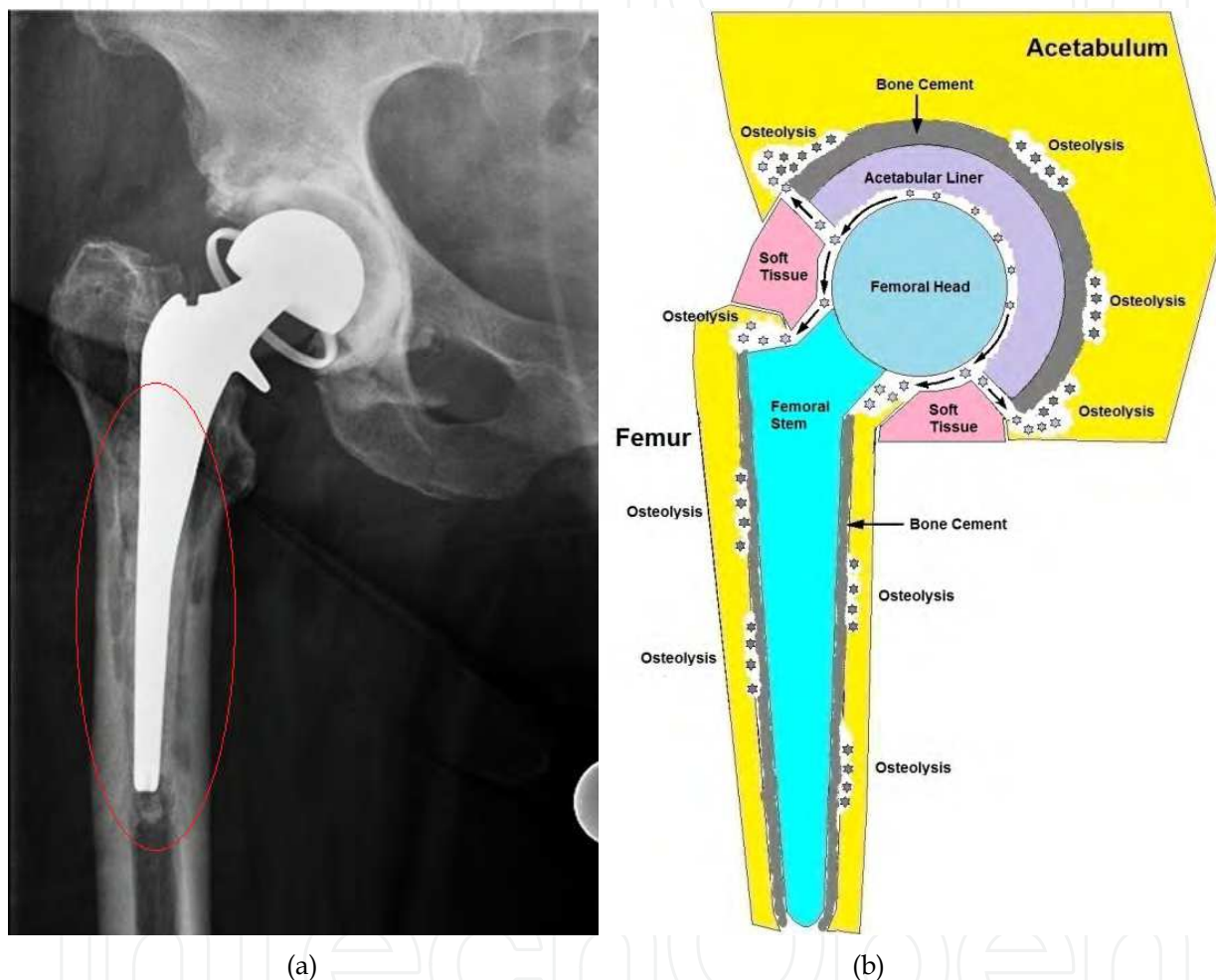


Fig. 1. (a) Radiograph of a cemented hip prosthesis with osteolysis around the femoral stem due to cement fragmentation (radiolucent areas within the red circled area surrounding the femoral stem). (b) Diagram of a cemented hip prosthesis with osteolysis around the acetabular and femoral implants. Wear particles are represented by small hexagonal stars, and in the illustration, are produced primarily from the acetabular liner (light gray stars liberated from the inner, articulating surface) and bone cement around the acetabular liner and femoral stem (dark gray stars liberated from fragmented cement). Interfaces between implant, bone, and cement serve as conduits for particle migration, as represented by the arrows. Particles can also be produced by the femoral head and stem, which are respectively made of cobalt chromium and titanium alloys. The acetabular liner is most often made of UHMWPE, and in most cases is the main source of wear particles.

shown that surface contact of macrophage membrane with particles of non-phagocytosable size ( $> 20 \mu\text{m}$ ) is sufficient to trigger an inflammatory response; however, the response elicited is much smaller than that triggered by particle phagocytosis. Other cells recruited to the site of osteolysis include migrated monocyte/macrophages, neutrophils, and lymphocytes; however, it is the macrophage that plays the dominant role in this inflammatory response. *In vitro* studies have used macrophages from primary sources such as murine peritoneal macrophages and human peripheral blood monocytes, or immortalized cell lines such as Raw267.4 and J774 macrophages. Macrophages are activated by all particle types including titanium, polyethylene, and PMMA, and have in nearly all cases been documented to release cytokines in a dose-dependent manner, with particles in the size range of 0.5 to 10  $\mu\text{m}$  yielding the highest inflammatory response.

Besides invoking inflammation, wear debris particles also indirectly promote the formation and activity of osteoclasts, the primary cells that mediate bone resorption. After phagocytosing particles, macrophages secrete the osteoclastogenic factors RANKL and M-CSF. Furthermore, fibroblasts, osteoblasts, and marrow stromal cells are also capable of phagocytosing particles and releasing RANKL and M-CSF. These two factors stimulate monocyte-macrophage precursors of hematopoietic lineage to differentiate into pre-osteoclasts, which then fuse to become mature osteoclasts capable of resorbing bone and showing phenotypes such as multinucleation and expression of TRAP (tartrate resistant acid phosphatase). Monocytes respond to RANKL via the surface receptor RANK. Monocytes may be resident in peri-implant tissue or recruited from peripheral blood. The ability of monocytes to form bone-resorbing osteoclasts after being challenged with wear debris particles has been well documented with human peripheral blood monocytes and mouse peritoneal macrophages exposed directly to particles *in vitro*, treated with RANKL and M-CSF, cocultured with particle-treated macrophages, osteoblasts, or marrow stromal cells, or grown in conditioned medium taken from these particle-treated cell cultures. This osteoclastogenic effect is seen with all particle materials, including polyethylene, titanium, and PMMA. A series of studies has shown that osteoclast differentiation from mouse monocytes co-cultured with UMR-106 osteosarcoma cells is potentiated by PMMA particles, as indicated by increased numbers of TRAP-positive cells and resorbed pits in co-cultured bone slices, compared to control monocytes not exposed to PMMA particles (Sabokbar et al., 1996, 1997, 1998). This enhanced osteoclastogenic response was also documented in a similar study which showed that mouse monocytes grown in osteoclastogenic medium containing M-CSF and RANKL yielded higher numbers of TRAP-positive multi-nucleated cells and resorbed pits in co-cultured bone slices when treated with PMMA particles, compared to monocytes grown in the same system but not exposed to PMMA particles (Zhang et al., 2008). Another series of studies has shown that enhanced osteoclastogenesis of mouse monocytes in medium containing M-CSF and RANKL after exposure to PMMA particles involves increased expression and activity of NF- $\kappa$ B (Clohisy et al., 2006), MAP kinases p38, ERK, and JNK (Abbas et al., 2003; Yamanaka et al., 2006), and the transcription factor NFAT (Yamanaka et al., 2008); these enhanced osteoclastogenic responses were respectively abrogated by inhibitors against NF- $\kappa$ B, the MAP kinases, and NFAT. A similar study has also demonstrated that titanium particles enhance NFAT expression in monocyte-derived osteoclasts in medium containing M-CSF and RANKL, a process that was also disrupted using an inhibitor against NFAT (Liu et al., 2009). Osteoclasts are also regulated by osteoblasts, which are a major source of OPG (osteoprotegerin), a soluble receptor that

binds to RANKL and prevents it from binding RANK on monocytes. OPG is normally secreted by osteoblasts to inhibit osteoblast formation and activity.  $\text{TNF-}\alpha$ , IL-1, and  $\text{PGE}_2$  increase expression of RANK on monocytes and reduce expression of OPG in osteoblasts. The intracellular effects of RANKL-RANK binding are mediated by the master transcription factor  $\text{NF-}\kappa\text{B}$ . The prevention of RANKL-RANK interactions by knockout methods in mice or by administration of a RANKL antagonist abolishes the osteolytic response to orthopaedic wear particles. IL-1 is another factor important for formation and activity of osteoclasts. Knockout of IL-1 receptors, IL-1RI and IL-1RII, in mice or administration of IL-1 receptor antagonists, also abolishes osteolytic response to particles.

Wear debris also causes the formation of a fibrous, granulomatous tissue membrane around the loosened prosthesis (Goodman, 1994). The membrane stroma is formed from fibroblasts and serves as a support structure for macrophages, osteoblasts, osteoclasts, lymphocytes, and multinucleated/foreign body giant cells. This fibrous membrane is formed from micro-movements at the bone-implant interface, and not only harbours these cells, but serves as a conduit for particle migration and inflammatory mediators. Granulomas in the membrane are clusters of macrophages and fibroblasts mixed within collagen deposits, and represent an attempt to wall off foreign material that it cannot destroy. Tissues retrieved from failed implants and cultured in vitro release high quantities of  $\text{TNF-}\alpha$ , IL-1, IL-6, IL-8,  $\text{PGE}_2$ , RANKL, M-CSF, MCP-1, MMPs, collagenases, the same factors released by macrophages, osteoblasts, osteoclasts, and fibroblasts when treated individually with particles in vitro. In vitro fibroblast studies have been conducted with primary human or mouse foreskin and synovial fibroblasts, mouse calvarial and neonatal fibroblasts, and fibroblast cell lines. Fibroblasts produce the same inflammatory and osteoclastogenic factors as macrophages and osteoblasts, such as IL-6, RANKL,  $\text{PGE}_2$ , which are capable of stimulating osteoclast formation in co-cultures with monocytes.

Metal particles can potentially exert a toxic ion effect on cells. Unlike polyethylene and ceramics, metals such as titanium, cobalt chromium, and stainless steel potentially dissolve into metal ions, albeit very slowly. The high surface area-volume ratio of the predominantly nanometer-sized metal particles facilitates their dissolution into ions. Metals can also undergo corrosion and oxidation, especially in the physiological environment of the body. Aluminium, vanadium, and nickel in alloys also have the potential to produce small particles and ions. High concentrations of metal ions have been detected in joint fluid and tissues retrieved from failed implants. These metal ions may trigger a cytotoxic or hypersensitivity reaction from tissues in vivo. Metal hypersensitivity has been reported to be as high as 50-60% in patients with failed implants, whereas it is only 10-15% in the general population. Metal ion toxicity has been demonstrated in vitro with metal salts such as  $\text{CoCl}_2$ ,  $\text{CrCl}_3$ , and  $\text{CrCl}_6$ , on murine macrophages and osteoblasts, which show reduced cell viability. In these studies, cobalt ions have proven to be the most toxic, while ions of titanium, chromium, and aluminum are relatively well tolerated. Metal ions can remain in body fluid as soluble ions, precipitate as insoluble metal salts or oxides, chelate with organic anions to form organometallic complexes, or be stored and transported by carriers like hemosiderin. Elevated ion levels may be detected in local tissue, serum, and urine; they may also be transported to distant organs via the bloodstream. The organs of patients with failed implants show high levels of cobalt and chromium in serum, liver, spleen, kidney, and lymphatic tissues. Cobalt chromium alloy is most resistant to wear and corrosion (it

dissolves at a linear rate of about 50 nm per year), while stainless steel corrodes more easily. Titanium alloy is softer and wears more easily, hence it is not used as articulating surface but as stem components. Inflammation and osteolysis of implants yields a locally acidic environment which accelerates the rate of wear and corrosion. Although in vivo studies in rats and dogs have shown that cobalt chromium and stainless steel implants yield a slightly higher incidence of sarcomas, this has not been demonstrated in humans. Chronic metal ion toxicity may be exacerbated in the presence of renal failure.

Immune reactions associated with wear debris particles can be augmented by the presence of bacterial lipopolysaccharides (LPS) or endotoxin, which are molecules that can independently induce inflammation (Greenfield et al., 2008). Endotoxin adheres to implant surfaces, and may be introduced into the joint by contaminated implants or via circulation from distant sites of infection. Endotoxin may accumulate on the implant and accelerate the process of inflammation and osteolysis. Monocyte macrophages, in particular, respond to endotoxin by releasing pro-inflammatory mediators and inducing osteoclast formation and activity. Osteoblasts respond to endotoxin with diminished proliferation, collagen synthesis, and differentiation. Endotoxin has been found in tissues of failed implants, more frequently in patients with inflammatory arthritis such as rheumatoid arthritis.

#### 4. Biological response of osteoblasts

Osteoblasts in peri-implant tissue deposit bone and are responsible for ensuring osseointegration of the implant. Continual exposure of osteoblasts to wear particles impairs their function and shifts bone metabolism in favor of increased bone resorption and decreased bone formation. In vitro studies have shown that implant wear debris not only induces inflammatory, osteolytic, and granulomatous reactions, but also affects osteoblasts by disrupting their proliferation, survival, adhesion, extracellular matrix synthesis, and cytokine release profile. These results have been demonstrated with metal, polyethylene, cement, and ceramic particles on osteoblasts from primary sources and osteoblast cell lines. Osteoblasts can phagocytose particles less than 10  $\mu\text{m}$  in size. Internalized particles cause damage to intracellular organelles and disrupt cytoskeletal networks, leading to cell death and loss of ability to proliferate and synthesize matrix proteins such as collagen and proteoglycans. Osteoblasts normally interact with osteoclasts in a delicate balance via secreted factors RANKL and OPG, but during inflammatory states induced by particles, they secrete higher levels of RANKL, inflammatory mediators such as IL-6 and PGE<sub>2</sub>, and chemokines such as IL-8 and MCP-1. The response of osteoblasts to particles differs according to particle size, shape, material composition, and number, and the maturational state of the osteoblast. Table 1 summarizes the findings of selected in vitro osteoblast studies.

Orthopaedic wear particles less than 10  $\mu\text{m}$  in size are universally phagocytosed by osteoblasts. Although cell surface contact with particles of non-phagocytosable size (e.g., > 20  $\mu\text{m}$ ) is reported to elicit some degree of inflammation from osteoblasts, the adverse reactions of osteoblasts to phagocytosable particles is much greater. Particle phagocytosis is generally regarded as the first step for triggering adverse reactions from these cells, as all studies involving osteoblasts and implant particles less than 10  $\mu\text{m}$  have reported phagocytosis (Pioletti et al., 1999, 2002; Vermes et al., 2001; Yao et al., 1997). Particle

Author	Year	Particle (Size)	Cell Type	Outcomes
Allen	1997	CoCr (14.37 ± 5.89 µm) Co (4.75 ± 4.16 µm) Cr (1.89 ± 1.58 µm)	MG63, SaOS-2	alkaline phosphatase (↓), osteocalcin (↓), viability (↓ for Co only), collagen I (↓ for Co only)
Yao	1997	Ti (91% < 3 µm) Ti (21.85 µm)* PolS (1.14 ± 0.007 µm) PolS (21.1 ± 4.09 µm)*	MG63, HOS	procollagen I and III (↓), collagen I (↓), proliferation (-), viability (-), particle phagocytosis(+)
Martinez	1998a	UHMWPE (20-200 µm)*	PHO	procollagen I (↓), alkaline phosphatase (↑), osteocalcin (↑)
Martinez	1998b	UHMWPE (< 160 µm)*	PHO	proliferation (↓)
Zamboni	1998	PMMA (70% < 10 µm)	PHO	proliferation (↓), collagen I (↓), osteocalcin (↑), IL-6 (↑)
Dean	1999a	UHMWPE (90% < 1.5 µm)	MG63	proliferation (↑), collagen (↓), alkaline phosphatase (↓), osteocalcin (↓), proteoglycan (↓), PGE2 (↑)
Dean	1999b	UHMWPE (1.0 ± 0.96 µm)	MG63	proliferation (↑), alkaline phosphatase (↓), proteoglycan (↓), PGE2 (↑), TGFβ1 (↓), osteocalcin (-)
Pioletti	1999	Ti (3.1 ± 3.6 µm)	RatNC	viability (↓), particle phagocytosis (+), apoptosis (+), soluble cytotoxic factors
Heinemann	2000	Ti6Al4V (1-3 µm)	PHO, MG63	particle phagocytosis (+)
Kwon	2000	Ti (80% < 5 µm, 1-10 µm)	RatNC	adhesion (↓)
Lohmann	2000	Ti (0.81 ± 0.12 µm) Ti6Al4V (1.35 ± 0.09 µm) CoCr (1.21 ± 0.16 µm) UHMWPE (1.0 ± 0.96 µm)	MG63, PHO	alkaline phosphatase (↓), PGE2 (↑), intracellular organelle damage (+), proliferation (↑ for MG63)
Shida	2000	Ti (1-3 µm)	MG63	IL-6 (↑), particle phagocytosis (+), NF-κB and NF-IL-6 binding (+)
Takei	2000	Ti (80% < 5 µm)	MG63, SaOS-2	proliferation (↓), alkaline phosphatase (↓), IL-6 (↑), conditioned medium effect (-)
Vermes	2000	Ti (1-3 µm) Ti6Al4V (90% < 3 µm) UHMWPE (90% < 3 µm) PolS (1.14 ± 0.01 µm) Ti (21.85 µm)* PolS (21.1 ± 4.1 µm)*	MG-63, PHO SaOS-2, HOS	procollagen I and III (↓), collagen I (↓), IL-6 (↑), particle phagocytosis (+), NF-κB binding (↑), TNF-α (-), IL-1α (-), IL-1β (-), osteonectin (-), osteocalcin (-), alkaline phosphatase (-)
Dean	2001	UHMWPE (0.46-1.26 µm)	MG63	proliferation (↑), PGE2 (↑), alkaline phosphatase (↓)
Kwon	2001	Ti (80% < 5 µm, 1-10 µm)	RatNC	adhesion (↓), proliferation (↓)
Roebuck	2001	Ti (94% < 3 µm)	MG63	NF-κB binding (↑), PI3K activity (↑)
Rodrigo	2001	UHMWPE (20-200 µm)**	PHO	procollagen (↓), alkaline phosphatase (-)
Vermes	2001	Ti (1-3 µm) Ti6Al4V (90% < 3 µm) UHMWPE (90% < 3 µm) PolS (1.14 ± 0.01 µm)	MG63	procollagen I (↓), proliferation (↓), IL-6 (↑), viability (-), particle phagocytosis (+), TNF-α (-), IL-1 (-), osteonectin (-), osteocalcin (-), alkaline phosphatase (-)
Fritz	2002	Ti (94% < 3 µm)	MG63, PHO	IL-8 (↑), MCP-1 (↑), NF-κB binding (↑)
Lohmann	2002a	UHMWPE (1.0 ± 0.96 µm)	MG63, OCT1, MLO-Y4	PGE2 (↑), osteocalcin (-), proliferation (↑ for MG63, - for OCT1, ↓ for MLO-Y4), NO production (- for MG63, ↑ for OCT1, ↑ for MLO-Y4)
Lohmann	2002b	PMMA (2.22 ± 0.07 µm) Al2O3 (1.09 ± 0.15 µm) ZrO2 (1.84 ± 0.04 µm)	MG63	PGE2 (↑), proliferation (↓ for Al2O3, ↑ for ZrO2 and PMMA), alkaline phosphatase (↓ for Al2O3, ↑ for ZrO2 and PMMA)
Pioletti	2002	Ti (10% < 10 µm)* PMMA (10% < 10 µm)*	MG63, SaOS2, RatNC	apoptosis (+), particle phagocytosis (+), cytoskeletal disruption (+)
Rodrigo	2002	HDPE (< 5 µm) Al2O3 (< 5 µm)	PHO	IL-6 (↑)
Granchi	2004	UHMWPE (0.1-1.0 µm) Al2O3 (1.0 µm mean)	PHO	IL-6 (↑), RANKL (↑), OPG (↓ for UHMWPE, ↑ for Al2O3), GM-CSF (-), TNF-α (-), viability (-)
O'Conner	2004	Ti (< 1.5, 1.5-4, 5-9 µm)	RatNC	proliferation (↓), viability (↓), particle phagocytosis (+), cytoskeletal disruption (+)
Pioletti	2004	Ti (4.5 µm mean)	PHO	RANKL and CSF-1 (↑), OPG (-)
Ciapetti	2005	FeAlCr (3.4-7.5 µm) Ti6Al4V (150 µm mean)	SaOS-2	particle phagocytosis (+), viability (↓), proliferation (↓), Al and Cr ion (+)
Fritz	2005	Ti (94% < 3 µm)	MG63	NF-κB binding (↑), ERK1/2 and JNK 1/2 activation (↑)
Granchi	2005	UHMWPE (0.1-1.0 µm) Al2O3 (1.0 µm mean)	PHO	RANKL (↑ for UHMWPE only), OPG (↓ for UHMWPE only)
Peter	2005	Ti (4.5 µm mean)	MG63, MC3T3E1	alkaline phosphatase (↓)
Friz	2006	Ti (94% < 3 µm)	MG63, PHO	IL-8 (↑), MCP-1 (↑), NF-κB binding (↑)
Ramachandran	2006	Ti (4-10 µm) PMMA (1-10 µm)	MG63	NO production (-), viability (-), alkaline phosphatase (-), osteocalcin (-)
Valles	2008	Ti (3.32 ± 2.39 µm) TiO2 (0.45 ± 0.26 µm)	PHO	IL-6 (↑), PGE2 (↑), RANKL (-), OPG (+/-), GM-CSF (+/-), viability (-)
Kanaji	2009	CoCrMo (0.5-10 µm)	MLO-Y4	TNF-α (↑), IL-6 (↓), caspase-3 and caspase-7 (↑)
Lenz	2009	Ti (3 µm mean) ZrO2 (1.75 ± 4.66 µm) Ti6Al7Nb (3.46-4.44 µm mean) CoCrMo (2.81-3.24 µm mean)	PHO	viability (↓), collagen I (↓)

Table 1. Summary of implant particle effects on osteoblasts. Studies are listed in in chronological order. Abbreviations: Ti = titanium particles, Ti6Al4V = titanium alloy particles, UHMWPE = ultrahigh molecular weight polyethylene particles, PMMA = polymethylmethacrylate particles, CoCr (CoCrMo) = cobalt chromium alloy particles, PolS= polystyrene particles, Al2O3 = aluminium oxide/alumina particles, ZrO2 = zirconium oxide/zirconia particles, FeAlCr= iron alloy particles, HDPE = high density polyethylene particles, TiO2 = titanium oxide (rutile) particles, RatNC = neonatal rat calvarial osteoblasts, PHO = primary human osteoblasts. Osteoblast cell lines are represented as MG-63, SaOS-2,

HOS, OCT-1, MLO-Y4. Signs: (↓) indicates decrease, (↑) indicates increase, (+) indicates presence of, (-) indicates no change, (+/-) indicates small increase, asterix \* indicates particles are of non-phagocytosable size.

internalization can be visualized using fluoresceinated particles such as Fluoresbrite (polystyrene-based fluorescent particles). Fluoresbrite particles have been used to demonstrate that phagocytosis occurs mostly within 24 hours of *in vitro* exposure, and that cells become saturated with these particles ( $0.926 \pm 0.027 \mu\text{m}$  in size) at 40-60 particles/cell, a quantity that can be determined by plotting the fluorescence of particles extracted from lysed cells against a fluorescence intensity standard curve of known Fluoresbrite numbers (Vermes et al. 2001). Fluorescence and transmission electron microscopy and energy-dispersive x-ray analysis have been used to reveal that osteoblasts with internalized particles have evidence of damage to cell membranes, mitochondria, endoplasmic reticulum, and Golgi bodies, and ultrastructural changes indicative of cytotoxicity (Lohmann et al., 2000, 2002b). These morphological changes have been observed with titanium, titanium alloy, cobalt chromium alloy, UHMWPE, PMMA, and alumina particles. Fluorescence microscopy has been used to visualize the organization of actin filaments stained with rhodamine phalloidin assembled around internalized implant particles, as compared to healthy cells in which actin filaments organize around the nucleus (Kwon et al., 2000). The requirement of phagocytosis is proven with the use of cytochalasin D, a fungal substance that prevents actin filament assembly, a process required for cell division, phagocytosis, and formation of cytoplasmic extensions. Osteoblasts pre-treated with cytochalasin D at 1-5  $\mu\text{M}$  are prevented from phagocytosing particles and show lower degrees of IL-8 release (Fritz et al., 2006), cytotoxicity and apoptosis (Pioletti et al., 1999), and inhibition of procollagen type I expression (Vermes et al., 2000, 2001) compared to particle-treated osteoblasts not exposed to cytochalasin D. Phagocytosed particles can also be visualized by confocal microscopy (Valles et al., 2008; Yao et al., 1997); light and phase contrast microscopy can be used to crudely visualize particles floating within individual cells in cell culture or suspension. Particles of non-phagocytosable sizes induce lower degrees of adverse effects from osteoblasts. Titanium particles  $> 20 \mu\text{m}$  for instance do not effectively inhibit collagen and procollagen synthesis as particles  $< 10 \mu\text{m}$  (Vermes et al., 2000; Yao et al., 1997). Studies have indicated that particles 0.1-1.0  $\mu\text{m}$  are most deleterious to osteoblasts. Scanning electron microscopy has revealed that particulate materials generated from implant wear vary more greatly in shape than commercially produced particles, and are more detrimental or inflammatory to osteoblasts. UHMWPE debris particles generated from wear simulator tests or retrieved from failed hip arthroplasties for instance, can be round, oblong, or thin and fibril-like, with irregular grainy surfaces (Dean et al., 1999b), while commercially produced polymeric particles such as PMMA or polystyrene, are mostly spherical.

Depressed type I collagen synthesis is universally observed in osteoblasts exposed to implant wear debris in MG-63, SaOS-2, human osteogenic sarcoma, and primary human osteoblasts treated with titanium, titanium alloy, cobalt chromium, PMMA, UHMWPE, or polystyrene particles (Dean et al., 1999a; Lenz et al., 2009; Vermes et al., 2000, 2001; Yao et al., 1997; Zambonin et al., 1998). These studies reveal a clear dose-dependent decrease in collagen mRNA and protein synthesis over at least a 72 hour period. The inhibitory effects on collagen are related to particle size and dose, but not to the material composition of the particles. Particles are reported to affect the production of other osteoblast proteins, though

these reports differ in whether particles inhibit or stimulate this process. A series of studies has reported that submicron-sized UHMWPE particles dose-dependently inhibit the production of alkaline phosphatase, osteocalcin, and proteoglycans (Dean et al., 1999a, 1999b, 2001). Another study with metal particles including titanium, titanium alloy, or cobalt chromium has shown that these materials dose-dependently reduce alkaline phosphatase activity in MG-63 and primary human osteoblasts (Lohmann et al., 2000). However, another series of studies did not report that particles of titanium, titanium alloy, UHMWPE, or polystyrene affected the production of alkaline phosphatase, osteocalcin, or osteonectin in MG-63, SaOS-2, or primary human osteoblasts (Vermes et al., 2000, 2001). Yet other studies have shown that these responses vary with particle material composition; for instance, these studies have shown that PMMA particles increase production of alkaline phosphatase and osteocalcin respectively in MG-63 cells and primary human osteoblasts (Lohmann et al., 2002b; Zambonin et al., 1998), and that alumina particles decrease while zirconia particles increase alkaline phosphatase production in MG-63 cells (Lohmann et al., 2002b).

Orthopedic wear particles are reported to affect the proliferation of osteoblasts. However, reports differ as to whether particles inhibit or stimulate their proliferation. One study reported that proliferation of MG-63 osteoblasts was inhibited dose-dependently when treated with titanium, titanium alloy, UHMWPE, and polystyrene particles (Vermes et al., 2001); other studies showed that titanium particles dose-dependently inhibited the proliferation of neonatal rat calvarial osteoblasts (Kwon et al., 2001) and MG-63 and SaOS-2 osteoblasts over a 72 hr period (Takei et al., 2000). The inhibitory effects of titanium particles were stronger on SaOS-2 cells than MG-63 cells (Takei et al., 2000), suggesting that different maturational states affected the degree of sensitivity to particles. PMMA particles were also shown to decrease proliferation of primary human osteoblasts (Zambonin et al., 1998). Some studies however, reported that wear particles stimulated osteoblast proliferation. A series of studies demonstrated that submicron-sized UHMWPE wear particles from failed hip arthroplasties and GUR 4150 wear tests increased dose-dependently the proliferation of MG-63 cells (Dean et al., 1999a, 1999b, 2001). Another study demonstrated that titanium, titanium alloy, cobalt chromium, and UHMWPE particles increased proliferation of MG-63 osteoblasts in a dose-dependent manner (Lohmann 2000). Yet other studies showed that the effects of particles on proliferation varied with particle composition and size, and cell type and maturational state. One such study showed that when challenged with submicron-sized UHMWPE debris, proliferation increased for MG-63 (immature osteoblasts), remained unaffected for OCT-1 (mature secretory osteoblasts), and decreased for MLO-Y4 (osteocytes) cells (Lohmann et al., 2002a). Another study showed that proliferation of MG-63 cells was dose-dependently decreased by alumina particles and increased by PMMA and zirconia particles (Lohmann et al., 2002b). Yet another study showed that UHMWPE particles of higher molecular weight induced proliferation of MG-63 cells more readily than those of lower molecular weight (Dean et al., 2001). The different results for particle effects on proliferation may be due to differences in cell type, maturational state, passage number, health condition, and particle material, size, shape, and dose, as well as specific protocols for the experiments by different groups.

Wear particles are reported to impair osteoblast viability and adhesion. One study has shown that titanium particles dose-dependently decrease the viability of neonatal rat calvarial osteoblasts over 72 hrs (O'Conner et al., 2004; Pioletti et al., 1999, 2002), with

evidence of elevated caspase-3 activity and DNA fragmentation indicative of apoptosis (Pioletti et al., 1999, 2002). When cytochalasin D is applied to these cells, the inhibition of particle phagocytosis reduces the amount of cytotoxic cell death (Pioletti et al., 1999). Other studies have shown that cobalt chromium particles cause elevated caspase-3 and -7 activity in MLO-Y4 osteocytes after 24 hrs (Kanaji et al., 2009), and titanium and iron alloy particles cause reduced viability and proliferation in SaOS-2 cells after 48 hrs. However, some studies did not detect significant reductions in viability in MG-63 or primary human osteoblasts exposed to titanium, UHMWPE, polystyrene, or alumina particles (Granchi et al., 2004; Valles et al., 2008; Vermes et al., 2001; Yao et al., 1997). Titanium particles are also reported to impair the adhesion of neonatal rat calvarial osteoblasts in a dose-dependent manner, conducted at the single cell level using a micropipette system to measure detachment force (Kwon et al., 2000), and the strength of osseointegration of titanium alloy rods in the rat tibia (Choi et al., 2005).

Implant wear debris induces osteoblasts to secrete inflammatory cytokines, chemokines, and osteoclastogenic factors, while downregulating growth factors that promote osteoblast growth or inhibit osteoclastogenesis. Osteoblasts exposed to implant particles release factors that promote the following processes: (1) inflammation mediated by IL-6, and PGE<sub>2</sub>, upregulated by transcription factor NF- $\kappa$ B activated after particle phagocytosis; (2) chemoattraction of inflammatory cells by IL-8 and MCP-1, which recruit neutrophils and monocyte-macrophages respectively (the latter are precursors to osteoclasts); (3) osteoclast formation and activation induced by M-CSF and RANKL, (the latter binding to the receptor RANK on monocytes, promoting their differentiation into osteoclasts) and diminished expression of OPG (osteoprotegerin) and TGF- $\beta$ 1, factors which suppress osteoclast activity; and (4) matrix degradation by matrix metalloproteinases MMP-2 and MMP-9, and collagenases. IL-6 released by osteoblasts potentiates bone resorption by recruiting osteoclasts and promoting their differentiation and activation. Implant particles activate NF- $\kappa$ B through increased degradation of I $\kappa$ B $\alpha$ , an inhibitor that binds to and prevents NF- $\kappa$ B from translocating from cytosol into the nucleus. Particles decrease osteoblast expression of TGF- $\beta$ 1, a growth factor that stimulates osteoblast proliferation and procollagen I expression and inhibits osteoclastogenesis (Dean et al., 1999b).

Studies universally show that osteoblasts release cytokines that promote inflammation and osteoclastogenesis after exposure to wear particles. RANKL and CSF-1 production by primary human osteoblasts is induced by titanium particles after 24-48 hours of treatment (Pioletti et al., 2002). IL-6 and PGE<sub>2</sub> are released from primary human osteoblasts after exposure to titanium and titanium alloy (Valles et al., 2008; Vermes et al., 2000, 2001), PMMA (Zambonin et al., 1998), and alumina (Rodrigo et al., 2002) particles. Two series of studies have confirmed that UHMWPE particles induce the release of PGE<sub>2</sub> from MG-63 (Dean 1999a, 1999b, 2001), OCT-1, and MLO-Y4 cells (Lohmann et al., 2002a). One of these series has also shown that MG-63 cells release PGE<sub>2</sub> in a dose-dependent manner after exposure to titanium, titanium alloy, cobalt chromium, PMMA, alumina, and zirconia particles (Lohmann et al., 2000, 2002b). Chemokines IL-8 and MCP-1 are dose-dependently released from MG-63 and primary human osteoblasts treated with titanium particles (Fritz et al., 2002, 2006). Some studies, however, have reported that osteoblasts challenged with titanium particles do not release IL-1 or TNF- $\alpha$  (Vermes et al., 2000, 2001) or show no changes in secretion of GM-CSF, RANKL, or OPG unless at high particle doses (Valles et al., 2008). Studies have shown that adherent peripheral blood mononuclear cells (PBMCs)

grown in conditioned media taken from osteoblasts treated with UHMWPE particles, are associated with greater numbers of TRAP-positive, multinucleated cells indicative of osteoclasts compared to PBMCs grown in media from control cells not treated with particles, or in media from cells treated with alumina particles (Granchi et al., 2004, 2005). Medium from control cells also induces osteoclast formation, albeit to a lesser extent. ELISA analysis indicates that the OPG-to-RANKL ratio is significantly lower in medium from UHMWPE-treated cells (lower OPG-to-RANKL ratio favors osteoclast formation) compared to that from alumina-treated cells, which is about the same as the OPG-RANKL ratio from control cell medium (Granchi et al., 2004). This induction of osteoclast formation by conditioned media is blocked by anti-RANKL antibodies. OPG levels were negligible (below detectable limits) in UHMWPE-challenged cultures, but remained high in control cell and alumina-treated cultures (Granchi et al., 2004).

Wear debris activates NF- $\kappa$ B and protein tyrosine kinase (PTK) in osteoblasts as the pathway to inflammation and inhibition of collagen synthesis. Titanium particles activate NF- $\kappa$ B nuclear translocation and binding to gene promoters, and induce phosphorylation of PTK at 2 hours post-exposure to titanium particles, as indicated by presence of NF- $\kappa$ B binding complexes and tyrosine-phosphorylated proteins on western blot (Vermes et al., 2000). These studies did not reveal the involvement of alternate pathways such as protein kinase A or C in particle-mediated effects, as inhibitors of these pathways did not affect gene expression. On the other hand, inhibitors of PTK such as genistein, and of NF- $\kappa$ B such as PDTC (pyrrolidine dithiocarbamate), abolish the inhibitory effect of titanium particles on collagen expression in MG-63 and primary human osteoblasts, indicating that PTK and NF- $\kappa$ B mediate particle suppressive effects (Vermes et al., 2000). Large, non-phagocytosable particles ( $> 20 \mu\text{m}$ ) also cause some degree of NF- $\kappa$ B binding, confirming the original observation that cell surface contact mediates minor adverse effects. Another series of studies has shown that NF- $\kappa$ B activates IL-8 expression in MG-63 and primary human osteoblasts after titanium particle exposure (Fritz et al., 2002, 2005). Titanium particles induce expression of NF- $\kappa$ B subunit p65 (RelA) and to a minor extent subunit p50 (NF- $\kappa$ B1). Gel shift mobility assays reveal binding of p65 and p50 to the IL-8-specific promoter an hour after particle exposure. The addition of an inhibitor of NF- $\kappa$ B, N-acetyl-L-cysteine, prevents p65 and p50 binding to the IL-8 promoter and leads to decreased production of IL-8. Titanium particles also activate the mitogen-activated kinase (MAPK) pathways ERK1/2 (p44/p42) and JNK1/2 (p54/p46) within minutes of particle challenge (Fritz et al., 2005). The pre-treatment of osteoblasts with MAPK inhibitors U0126 and SB203580 abolished the activity of ERK and p38, and concomitantly reduced the production of IL-8 (Fritz et al., 2005). Another study confirmed the role of NF- $\kappa$ B and PTK in reduction of collagen synthesis in MG-63 cells challenged with titanium particles (Roebuck et al., 2001). Titanium particle exposure led to upregulation of p65 and p50 and activation of PTK pathway, concurrent with suppressed type I collagen synthesis. Addition of the NF- $\kappa$ B inhibitor PDTC, or the PTK inhibitor genistein or herbimycin A, reduced the inhibitory effects expression and established the role of these pathways in mediating particle effects. On the other hand, inhibitors of protein kinase A and C did not influence the effects of particles on collagen expression, indicating that these pathways were not involved. These studies revealed the role of NF- $\kappa$ B and PTK as the mediators of downstream events of inflammation and diminished collagen synthesis that follow particle phagocytosis.

Metal wear debris has the additional issue of ion toxicity due to its potential to dissolve and corrode with time. Metal wear debris is on the scale of nanometers in size (mean, 50 nm), which is about 10x smaller than the average size of polyethylene particles (mean, 0.5  $\mu\text{m}$ ). The smaller size of metal particles increases their surface area for dissolution. Studies have shown that titanium and iron alloy (Ti-Al-V, Fe-Al-Cr) particles liberate aluminum and chromium ions into culture media in a dose-dependent manner, in addition to impairing viability and proliferation of tested SaOS-2 cells after phagocytosis (Ciapetti et al., 2005). A study evaluating the comparative cytotoxicity of cobalt, chromium, and cobalt-chromium alloy particles on MG-63 and SaOS-2 cells has shown that all three particle types inhibit alkaline phosphatase and osteocalcin expression, but cobalt particles inhibit these parameters to a much greater extent and are the only particles toxic enough to impair cell viability and type I collagen synthesis (Allen et al., 1997). Another study has shown that cobalt ( $\text{Co}^{2+}$ , 0-10 ppm) and chromium ( $\text{Cr}^{3+}$ , 0-150 ppm) ions generated from  $\text{CoCl}_2$  and  $\text{CrCl}_3$  are cytotoxic to MG-63 cells in a dose- and time-dependent manner over 72 hours, as

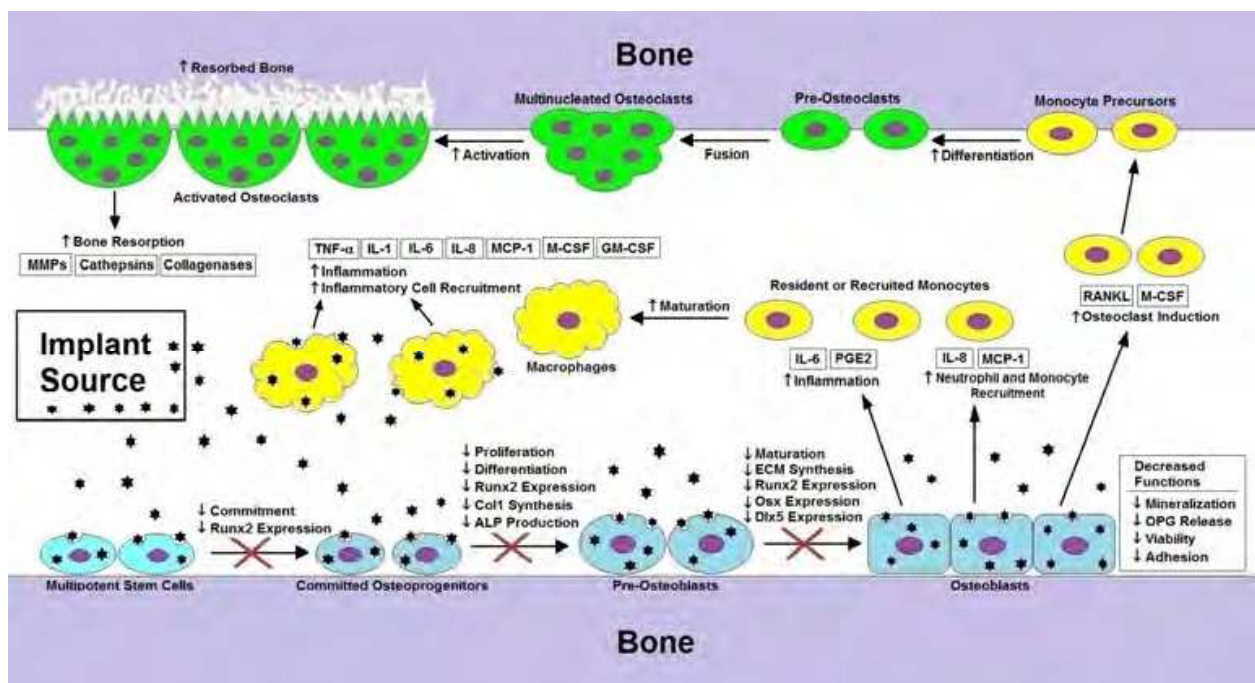


Fig. 2. Osteoblast-Osteoclast-Macrophage interactions during wear particle-induced inflammation and osteolysis. Small black hexagonal stars represent wear particles produced from the implant source. Bone-lineage cells (multipotent stem cells, osteoprogenitors, pre-osteoblasts, osteoblasts) are inhibited at each stage of development after phagocytosing wear particles. Osteoblasts release pro-inflammatory cytokines (IL-6,  $\text{PGE}_2$ ), chemoattractants (IL-8, MCP-1), and osteoclastogenic factors (RANKL, M-CSF) after exposure to particles. Resident macrophages also phagocytose particles and release a wide range of factors that mediate inflammation, osteoclast activation, and cell recruitment. Monocytes resident in local tissue or recruited from bloodstream mature into macrophages or differentiate into osteoclasts. RANKL and M-CSF produced from osteoblasts induce osteoclast formation and bone resorption. Activated osteoclasts produce matrix metalloproteinases, cathepsins, and collagenases, which degrade bone. ALP = alkaline phosphatase, Col1 = collagen I, Osx = osterix, ECM = extracellular matrix.

measured by MTT viability assay and cell count, with  $\text{Co}^{2+}$  being more cytotoxic than  $\text{Cr}^{3+}$  (Fleurry et al., 2006). Ion concentrations in this experiment however, are in the ppm range, and most likely beyond the physiological relevant range of ppb in fluids surrounding metal-on-metal prostheses. Another study, however, has shown that SaOS-2 cells incubated with  $\text{Co}^{2+}$ ,  $\text{Cr}^{3+}$ , and  $\text{Cr}^{6+}$  ions from chloride salts for 72 hrs, exhibited reduced viability only at doses far greater than physiological ranges in blood circulation ( $0.005 \mu\text{M}$ , or  $0.25 \mu\text{g/L}$ ). Specifically, SaOS-2 cells have shown decreased survival starting at  $10 \mu\text{M}$  for  $\text{Cr}^{6+}$  (the most potent of the three ions),  $100 \mu\text{M}$  for  $\text{Co}^{2+}$ , and  $450 \mu\text{M}$  for  $\text{Cr}^{3+}$  (Andrews et al., 2011). All three ion types have reduced alkaline phosphatase production and mineralization, but only at doses  $> 100 \mu\text{M}$ . Whether these ion doses are close to elevated levels of cobalt and chromium in synovial fluid of metal-on-metal prostheses needs to be determined. Yet another study has shown that  $\text{Co}^{2+}$  ions from  $\text{CoCl}_2$  induce primary human osteoblasts to release IL-8 and MCP-1, which causes the migration of neutrophils and macrophages in transwell experiments (Queally et al., 2011).  $\text{Co}^{2+}$  ions also significantly inhibit alkaline phosphatase production and calcium deposition in osteoblasts (Queally et al., 2011). These studies reveal that cobalt and chromium ions can be detrimental to osteoblasts, especially at elevated doses in peri-implant fluids of failed prostheses.

## 5. Biological response of osteoprogenitors

Bone formation involves bone and osteoid matrix deposition by osteoblasts and their differentiation from osteoprogenitors and multipotent stem cells, the latter being capable of differentiating along osteogenic, chondrogenic, and adipogenic pathways. These multipotent stem cells are often referred to as mesenchymal stem cells, which are defined as positive for mesenchymal markers CD27, CD44, CD90, CD105, CD166, and negative for hematopoietic markers CD34, CD45, and CD14. The term marrow stromal cells refers to the heterogeneous bone marrow cell population that remains adherent in tissue culture plates after removal of non-adherent blood cells. Within this marrow stromal cell population are multipotent stem cells, committed osteoprogenitors, fibroblasts, monocyte-macrophages, endothelial cells, and other undefined stromal support cells (Peister et al., 2004; Phinney et al., 1999). Upon exposure to osteoinductive factors, stem cells in this adherent culture commit to the osteogenic lineage. The osteoprogenitors undergo an initial period of proliferation, aggregation, and condensation, forming colonies that serve as the basis for subsequent osteoid matrix deposition (Lian & Stein, 2001). Osteoid production involves synthesis of type I collagen, proteoglycans, and glycosaminoglycans, and incorporation of osteonectin, osteocalcin, bone sialoprotein, and bone morphogenetic proteins (BMPs) into the matrix. Throughout this process, osteoprogenitors differentiate into pre-osteoblasts, which then mature into osteoblasts that can produce hydroxyapatite and bone. Once encased in bone matrix, osteoblasts turn into terminally differentiated, quiescent osteocytes. Osteoprogenitor differentiation is guided by the master transcription factor Runx2, which is required for expression of alkaline phosphatase, osteocalcin, collagen type 1, osteopontin, osteonectin, and bone sialoprotein. Another crucial transcription factor required for osteogenic differentiation is osterix (Osx), which is expressed by pre-osteoblasts and is downstream of Runx2 (Komori, 2006). Absence of Runx2 or osterix results in complete lack of osteogenesis (Komori, 2006). Two homeobox domain transcription factors, Dlx5 and Msx2, also regulate osteogenesis (Komori, 2006). Dlx5 promotes osteogenic differentiation,

while Msx2 acts as a functional antagonist or repressor of Dlx5-mediated osteogenesis (Chiu et al., 2010; Komori, 2006). Signaling pathways that mediate osteogenic differentiation include the mitogen-activated protein kinase (MAPK) system, which involves p38, ERK1/2, and JNK as the main signalling molecules, and the BMP/Smad system, which involves Smad proteins 1, 5, and 8 as the transducers of extracellular signals from BMPs (Lian & Stein, 2001). In summary, osteogenic differentiation involves an initial period of progenitor cell proliferation, an intermediate stage of extracellular matrix production, and a final stage of mineralization. Throughout this process, stem cells differentiate sequentially into osteoprogenitors, pre-osteoblasts, osteoblasts, and osteocytes. Multiple signalling pathways such as those of the MAP kinases and Smad signalling molecules, mediate downstream expression of the transcription factors Runx2 and osterix, which are required for osteogenesis. Orthopaedic wear debris has been shown to inhibit the osteogenic differentiation of osteoprogenitors and stem cells with respect to proliferation, viability, transcription factor expression, and osteogenic protein production. Given that osteogenesis requires the production of functional osteoblasts from osteoprogenitors, the inhibition of osteoprogenitor differentiation and proliferation by implant wear debris also reduces bone formation.

The effects of orthopaedic wear debris on osteogenic differentiation have been demonstrated using human or mouse marrow stromal cells and pre-osteoblast cell lines. A series of studies has assessed the effects of titanium particles on human marrow stromal cells (hMSCs, called mesenchymal stem cells in these studies) taken from patients undergoing primary hip or knee arthroplasty (Okafor et al., 2006; Wang et al., 2002, 2003). The hMSCs are heterogeneous populations containing multipotent stem cells with osteochondrogenic potential. When grown in osteogenic medium containing ascorbic acid, dexamethasone,  $\beta$ -glycerophosphate, and vitamin D<sub>3</sub>, hMSCs undergo osteogenesis in 12 days and divide at a much greater rate than those grown in non-osteogenic medium. In these studies, hMSCs exposed to titanium particles showed a dose-dependent decrease in proliferation, type I collagen and bone sialoprotein synthesis, mineralization, and viability (Wang et al., 2002). Titanium particles induced apoptosis in hMSCs, as evidenced by DNA fragmentation, upregulation of tumor suppressor proteins p53 and p73, and nuclear condensation (Wang et al., 2003). Like osteoblasts, hMSCs phagocytosed particles and showed evidence of disrupted cytoskeletal network. Zirconia particles also reduced proliferation, mineralization, and viability of hMSCs in a dose-dependent manner, but to a lesser degree than titanium particles, and did not affect collagen and BSP production, indicating that zirconia was less detrimental than titanium (Wang et al., 2002, 2003). Titanium particles also inhibited alkaline phosphatase production and impaired adhesion after particle phagocytosis; pre-treating hMSCs with cytochalasin D, an inhibitor of actin polymerization, prevented phagocytosis and apoptosis, and reversed the detrimental effects on adhesion and alkaline phosphatase production (Okafor et al., 2006). Another study showed that cobalt chromium particles inhibited the proliferation of multipotent stem cells purified from human marrow stromal cells by flow cytometry (positive for CD44, CD90, CD105, and negative for CD34, CD45, CD14), and that these cells also phagocytosed particles (Schofer et al., 2008).

The inhibitory effects of wear particles on osteogenic differentiation have also been demonstrated with mouse marrow stromal cells (mMSCs) isolated from mouse long bones, and the MC3T3-E1 pre-osteoblast cell line. Like hMSCs, mMSCs are heterogeneous and

harbour a subpopulation of multipotent stem cells with osteochodrogenic ability. PMMA particles dose-dependently inhibited the proliferation, alkaline phosphatase production, and mineralization of mMSCs, with complete suppression of these parameters observed throughout the entire culture period at particle doses  $\geq 0.150\%$  vol (Chiu et al., 2006, 2007). Exposure of mMSCs to PMMA particles for 5 days in either osteogenic or non-osteogenic medium was sufficient to make the inhibitory effects permanent; that is, removal of particles on or after 5 days of treatment did not halt or mitigate the inhibitory effects (Chiu et al., 2006, 2007). However, if particles were removed from culture before day 5 (e.g., on day 1 or 3), the inhibition of osteogenesis was partially mitigated (Chiu et al., 2007). In addition, PMMA particles were significantly less inhibitory when added to mMSC cultures at later days or stages of differentiation (e.g., days 5, 10, or 15 of culture) when the cells had mostly matured into osteoblasts (Chiu et al., 2006). PMMA particles also dose-dependently inhibited the proliferation, type I collagen and alkaline phosphatase expression, and mineralization of human multipotent stem cells purified from human bone marrow by flow cytometry (selected positively for CD27, CD44, CD106, CD166, and negatively for CD34, CD45, and CD14), with evidence of particle phagocytosis (Chiu et al., 2010b). MC3T3-E1 pre-osteoblasts challenged with PMMA particles exhibited a dose-dependent decrease in proliferation, alkaline phosphatase production, and mineralization (Chiu R et al., 2008; Ma et al., 2010). These effects were accompanied by particle phagocytosis, cytotoxic cell death, and importantly, the dose-dependent inhibition of osteogenic transcription factors Runx2, osterix, and Dlx5 (Chiu R et al., 2010a). Given that Runx2, osterix, and Dlx5 regulate osteogenesis, their inhibition likely caused downstream loss of osteoblast phenotype such as mineralization and alkaline phosphatase production. Interestingly, production of osteocalcin and expression of transcription factor Msx2 in MC3T3-E1 cells were not affected by PMMA particles. Msx2 is documented by certain studies as a reciprocal antagonist or repressor of Dlx5-mediated osteogenesis; hence, its lack of response to PMMA particles is consistent with the observed inhibition of Dlx5 and other osteoblast phenotypes. Another study investigated the pattern of mitogen-activated protein kinases (MAPKs), particularly p38, in MC3T3-E1 cells exposed to PMMA particles (Ma et al., 2010). MC3T3-E1 cells normally showed p38 activation on day 8 of osteogenic differentiation, but when exposed to PMMA particles, p38 was not activated on day 8, but instead on days 1 and 4 (Ma et al., 2010). The reasons for this changed pattern of p38 activation are unclear, but may involve a switch from an osteogenic program (p38 activation on day 8) to an inflammatory or apoptotic program (activation on days 1 and 4) given that p38 is involved in multiple signalling pathways. Lastly, MC3T3-E1 cells treated with titanium particles of nanometer size (mean size  $< 100$  nm) showed upregulated M-CSF production at about 3x the control levels within 48 hrs of particle exposure (Seo et al., 2007). This was accompanied by activation of another MAP kinase, ERK1/2, within 5 min of exposure to particles. Pre-treating MC3T3-E1 cells with an inhibitor of ERK1/2, PD98059, prevented ERK1/2 activation and concomitantly restored M-CSF secretion to control levels, which indicated that M-CSF expression was mediated by ERK1/2 signalling (Seo et al., 2007). The exposure of osteoprogenitors inhibited by implant particles to trophic or osteogenic growth factors moderately improved their osteogenic capacity. hMSCs inhibited by titanium particles, when exposed to IGF-1, FGF-2, BMP-6, and TGF- $\beta$ 1 at ng/mL concentrations, showed slightly enhanced proliferation, viability, and osteogenesis (Jeong et al., 2008). FGF-

Author	Year	Particle (Size)	Cell Type	Outcomes
Wang	2002	Ti (0.939 ± 0.380 μm) ZrO <sub>2</sub> (0.876 ± 0.540 μm)	hMSC	collagen I (↓), BSP (↓), viability (↓), proliferation (↓), mineralization (↓), particle phagocytosis (+), cytoskeletal disruption (+)
Wang	2003	Ti (0.939 ± 0.380 μm) ZrO <sub>2</sub> (0.876 ± 0.540 μm)	hMSC	viability (↓), apoptosis (+)
Chiu	2006	PMMA (1-10 μm)	mMSC	proliferation (↓), alkaline phosphatase (↓), mineralization (↓)
Okafor	2006	Ti (0.519 ± 0.125 μm)	hMSC	proliferation (↓), viability (↓), adhesion (↓), alkaline phosphatase (↓), particle phagocytosis (+)
Chiu	2007	PMMA (1-10 μm)	mMSC	proliferation (↓), alkaline phosphatase (↓), mineralization (↓)
Seo	2007	Ti (< 100 nm)	MC3T3E1	M-CSF (↑), ERK1/2 (↑)
Chiu	2008	PMMA (1-10 μm)	MC3T3E1	proliferation (↓), alkaline phosphatase (↓), mineralization (↓), osteocalcin (-)
Jeong	2008	Ti (1.46 ± 0.20 μm)	hMSC	slight to non-significant decreases in proliferation, viability, and collagen I, alkaline phosphatase, and osteocalcin; BSP (-)
Schofer	2008	CoCrMo (1.6-9.1 μm)	hMSC	proliferation (↓), particle phagocytosis (+)
Chiu	2009	UHMWPE (0.5 ± 0.2 μm)	mMSC MC3T3E1	proliferation (↓), alkaline phosphatase (↓), osteocalcin (↓), mineralization (↓)
Chiu	2010	PMMA (1-10 μm)	MC3T3E1	proliferation (↓), viability (↓), Runx2 (↓), osterix (↓), Dlx5 (↓), Msx2 (-), particle phagocytosis (+)
Chiu	2010	PMMA (1-10 μm)	hMSC	proliferation (↓), alkaline phosphatase (↓), collagen I (↓), mineralization (↓), particle phagocytosis (+)
Kann	2010	PMMA (1.10 μm)	MC3T3E1	alkaline phosphatase (↓), mineralization (↓)
Ma	2010	PMMA (1-10 μm)	MC3T3E1	mineralization (↓), alkaline phosphatase (↓), osteocalcin (-)

Table 2. Summary of orthopaedic particle effects on osteogenic differentiation of osteoprogenitor and marrow stromal cells. Studies are listed in chronological order. Abbreviations: Ti = titanium particles, UHMWPE = ultrahigh molecular weight polyethylene particles, PMMA = polymethylmethacrylate particles, CoCrMo = cobalt-chromium-molybdenum alloy particles, ZrO<sub>2</sub> = zirconium oxide particles, hMSC = human marrow stromal cells, mMSC = mouse marrow stromal cells, MC3T3E1 = MC3T3-E1 preosteoblasts. Signs: (↓) indicates decrease, (↑) indicates increase, (+) indicates presence of, (-) indicates absence of change.

2 and IGF-1 respectively enhanced proliferation and viability most effectively, increasing these two parameters in particle-treated cultures by 30-50% more than those not exposed to growth factors, and at levels beyond the control. FGF-2, IGF-1, and BMP-6 enhanced expression of type I collagen, alkaline phosphatase, osteocalcin, and BSP in the presence or absence of particles, with BMP-6 being most effective. However, titanium particles in this study had only slightly inhibited proliferation (by 10-15% relative to control), viability (by a non-significant 7%), and expression of collagen type I (38%), alkaline phosphatase (24%), and osteocalcin (15%), while not affecting expression of BSP (Jeong et al., 2008). The study also showed that TGF-β1 did not increase alkaline phosphatase, osteocalcin, or BSP expression and was the weakest of the four growth factors in terms of overall trophic effects on hMSCs. In another study, osteogenic protein-1 (OP-1), also known as BMP-7, improved the mineralization and alkaline phosphatase production of MC3T3-E1 pre-osteoblasts treated with PMMA particles. MC3T3-E1 cells exposed to PMMA particles showed a dose-dependent decrease in mineralization and alkaline phosphatase production, while the addition of OP-1 at 200 ng/mL to cultures significantly boosted these parameters by 30-170% at all time periods of treatment (days 1-20, 1-4, or 4-20 out of a 20-day culture period) and all particle doses tested (Kann et al., 2010). This increase in osteogenesis by OP-1 was significant whether particles were added to MC3T3-E1 cultures on the first or fourth day of growth. However, one study showed that the bisphosphonate zoledronate did not improve proliferation of MC3T3-E1 pre-osteoblasts or MG-63 osteoblasts in the presence of titanium particles (at 0.01% wt, the highest dose the cells could endure without showing signs of decreased proliferation relative to controls) throughout a 28 day period and over a wide dose range of zoledronate tested (0.1 to 100 μM by increasing orders of magnitude) (Peter et al., 2005).

## 6. *In Vitro* experimental methods

Most of our current knowledge of osteoblast and osteoprogenitor responses to orthopaedic wear debris comes from *in vitro* studies. These studies involve at a minimum, purifying and sterilizing particles and characterizing them with respect to size and shape, isolating and expanding cells and treating them with particles, and conducting various outcome measurements with respect to cell proliferation, differentiation, mineralization, viability, gene expression, protein or cytokine production, adhesion, or particle phagocytosis. With respect to gene expression and protein or cytokine production, commonly utilized methods include quantitative PCR after reverse transcription, Northern blot, *in situ* hybridization, and gene microarray analysis for mRNAs, and ELISA, western blot, immunohistochemistry, and enzyme reaction assays for proteins. Osteoblast proteins such as osteocalcin, bone sialoprotein, osteonectin, and osteopontin are commonly measured by ELISA or western blot. Alkaline phosphatase is commonly measured by enzyme kinetic reaction of cell lysates with para-nitrophenyl phosphate, its substrate, with spectrophotometric quantitation of chromogenic substrate release (p-nitrophenol) at 405 nm, or by immunohistochemistry given it is a cell surface protein. Secreted cytokines such as IL-6, IL-8, RANKL, M-CSF, and MCP-1 are often measured by ELISA of supernatant samples. All of these proteins can be measured by Q-PCR for mRNA expression. Transcription factors such as Runx2, osterix, Dlx5, and Msx2, are often measured by Q-PCR, while their binding to promoter elements in DNA is assessed by mobility shift electrophoresis, which separates protein-DNA complexes on gel. Mobility shift electrophoresis is also used to study the promoter binding activity of NF- $\kappa$ B subunits (RelA, NF- $\kappa$ B1), the transcription factor regulating particle-induced inflammation, cytokine production, and inhibition of collagen expression. Particle phagocytosis and ensuing morphological and cellular changes can be visualized by confocal, transmission electron, fluorescence, and light or phase contrast microscopy. Intracellular actin networks can be fluorescently visualized by staining with rhodamine or TRITC-conjugated phalloidin.

Calcium phosphate mineralization can be visualized by Alizarin Red S or von Kossa staining, measured by radioactive  $^{45}\text{Ca}$  incorporation, or by spectrophotometric quantification of o-cresolphthalein complexed with  $\text{Ca}^{2+}$  ions extracted from mineral nodules by 0.6 N HCl. Mineralized nodules in culture stained by the von Kossa method (incubation of fixed cultures in 5% silver nitrate under UV light for 30-60 min) can be quantified by NIH Imaging software and expressed as a percentage (total stained area over total culture well area) (Chiu et al., 2009). Mineralized nodules stained by Alizarin Red S can be quantified by spectrophotometrically measuring Alizarin Red dye extracted from mineralized nodules with 10% acetic acid (Gregory et al., 2004). Matrix collagen and proteoglycan content can be measured respectively by radioactive  $^3\text{H}$ -proline and  $^{35}\text{S}$ -sulfate incorporation.

Viability and proliferation are commonly measured outcomes of osteoblasts and osteoprogenitors in particle experiments. A variety of methods are used to assess viability: trypan blue exclusion, MTT assay, fluorescein diacetate uptake, Annexin V stain, LDH (lactate dehydrogenase) assay, and TUNEL or caspase-3 and 7 assays for apoptosis. Proliferation is assessed by cell counting,  $^3\text{H}$ -thymidine incorporation, BrdU uptake, and Ki67 antigen detection. Commercial sources also have proprietary kits/methods of assessing viability or proliferation (e.g., Alamar Blue, CCK-8 assay). Many of these assays are based

on the ability of viable cells to metabolize substrates (e.g., MTT, fluorescein diacetate, Alamar Blue) into chromogenic or fluorescent products for spectrophotometric measurement, or the ability of dividing cells to incorporate artificial nucleotides (e.g., BrdU,  $^{13}\text{H}$ -thymidine) which can then be detected. Other assays are based on the leakage of intracellular proteins during necrosis or cell injury (e.g., LDH), or specific events occurring in apoptosis (e.g., DNA fragmentation, phosphatidylserine inversion, caspase production). Many of these assays are available as commercial kits.

One of the initial steps of *in vitro* experimentation is obtaining a pure, sterile source of implant particles, either commercially or by isolating them from tissues of patients with failed hip or knee arthroplasties or wear simulator tests. Most studies with titanium, PMMA, or polystyrene particles have obtained these materials from commercial sources, most often Polysciences (Warrington, PA, USA) for PMMA and polystyrene particles, and Alfa Aesar (Ward Hill, MA, USA), now a part of Johnson Matthey, for titanium particles. Polysciences also produces fluorescent (Fluoresbrite) and color-dyed polystyrene particles, while Sigma-Aldrich (St. Louis, MO, USA) produces titanium oxide (rutile) particles. These particles are available in micron and submicron size ranges of phagocytosable size. Several studies have reported use of UHMWPE particles or powder from Hoechst-Celanese (Dallas, TX, USA) or its affiliated company Ticona (Florence, KY, USA), or Stryker-Howmedica-Osteonics (Kalamazoo, MI, USA) in various medical grades, such as GUR 4150. However, the UHMWPE powders obtained from these sources may be predominantly non-phagocytosable (i.e., 20-200  $\mu\text{m}$  in size) and must be filtered or subject to sedimentation to isolate particles of smaller size, with subsequent characterization by scanning electron microscopy to validate their actual size range. These particles can be sterilized by washing in 70% ethanol, autoclaving (for metal particles only), overnight UV light exposure, gamma irradiation, or ethylene oxide treatment.

UHMWPE wear debris is more often obtained from granulomatous membrane tissues or synovial fluid collected respectively from failed hip and knee arthroplasties during revision surgery or from serum lubricant in wear simulator tests (Campbell et al., 1995). Membranes are freshly stored in buffered formalin after retrieval, then minced into  $\text{mm}^3$  sized pieces, washed thoroughly with water, and digested in papain solution (3 mg papain in 10 mL of 50 mM phosphate buffer, pH 6.5, with 2 mM N-acetyl-L-cysteine) at 65° C for 1-3 days (Maloney et al., 1995; Wirth et al., 1999). Insoluble lysates are precipitated by centrifugation; the collected digest supernatant is then sonicated for 10 min and filtrated through a 0.2  $\mu\text{m}$  polyester filter to isolate the UHMWPE particles. The collected particles are washed with water and sterilized in 70% ethanol, then after final washing, stored in DMEM or saline for later addition to cultures (Maloney et al., 1995; Wirth et al., 1999). UHMWPE debris are retrieved from synovial fluid or wear serum by digesting these samples in 5-10 M sodium hydroxide solution for 12-24 hrs at 65° C (Affatato et al., 2001; Chiu et al., 2009; Minoda et al., 2004; Wolfarth et al., 1997). Serum samples may be lyophilized to dryness before digestion (Chiu et al., 2009). The digest supernatant is sonicated, then ultracentrifuged under a layer of 5% sucrose density gradient at high speed for 3 hrs at 4° C. The sucrose solution is collected and ultracentrifuged under a two-layered isopropanol-water density gradient (0.90, 0.96  $\text{g}/\text{cm}^3$ ) at high speed for 1 hour. The layer containing UHMWPE debris at the interface of the two volumes of isopropanol is collected, filtered through a 0.1  $\mu\text{m}$  polycarbonate filter, and allowed to dry. UHMWPE particles retrieved from patient samples and wear simulator tests are 1.0  $\mu\text{m}$  (0.2 to 1.5  $\mu\text{m}$ ) in size according to SEM analysis in

numerous reports. UHMWPE particles may be sterilized by gamma irradiation from a cesium-137 source, UV light exposure, 70% ethanol wash, or ethylene oxide treatment. Prior membrane fixation in formalin also destroys endotoxin and microbes. To confirm if the retrieved particles are UHMWPE, micro-Raman spectroscopy is used to generate a spectrum of vibrational frequencies from the particles that are matched with those of a UHMWPE standard reference (Wirth et al., 1999; Wolfarth et al., 1997; Visentin et al., 2004). Energy dispersive x-ray analysis provides spectra of elemental composition and can be used to identify metal (titanium, cobalt chromium) and ceramic (aluminium, zirconium) contaminants in the UHMWPE particle mixture (Affatado et al., 2001; Wolfarth et al., 1997; Maloney et al., 1995). Studies have shown with SEM that UHMWPE wear debris is mostly spherical or round, elongated, oval, or oblong, with rough, grainy surface containing numerous pits.

Particles should be sterilized and confirmed negative of bacterial endotoxin before addition to culture. Endotoxin induces many of the same biologic reactions as wear particles, including inflammation, cytokine production, and osteoclastogenesis, and potentiates the adverse effects of particles (Bi et al., 2001, 2002; Greenfield et al., 2005). Adherent endotoxin has been detected on commercial titanium particles and actual orthopedic implant materials as a result of the manufacturing process, can also originate from distant infections and accumulate on implants at subclinical levels, and are found at higher levels in patients with inflammatory arthritis such as rheumatoid arthritis (Bi et al., 2001; Nalepka et al., 2006; Greenfield et al., 2008). Endotoxins on particles or in supernatant can be measured using commercial assay kits, such as the Limulus Amoebocyte Lysate Kit from BioWhittaker (Walkersville, MD, USA). Endotoxin, if detected on metal particles, can be removed by five or more alternating cycles of incubation in 25% nitric acid at room temperature, then in 0.1 N sodium hydroxide in 95% ethanol at 30° C, each incubation for 18-20 hrs, with PBS washes in between each step (Ragab et al., 1999).

Osteoblasts may be obtained commercially as tumorigenic cell lines or from primary rodent or human sources. Osteoblast cell lines include MG-63, SaOS-2, U-2OS, HOS, OCT-1, and MLO-Y4, among which MG-63 is most popular. MG-63, SaOS-2, U2OS, and HOS cells are osteosarcoma (osteogenic sarcoma) cells derived from human patients, and show osteoblast traits of polygonal morphology, alkaline phosphatase and osteocalcin expression, collagen matrix deposition, and calcium phosphate mineralization. One study has described MG-63 as immature osteoblasts, and OCT-1 as mature secretory osteoblasts derived from the calvaria, and MYO-L4 as osteocytes derived from the long bones, of transgenic mice that express the SV40 T-antigen oncogene driven by the osteocalcin promoter (Lohmann et al., 2002a; Kato et al., 1997). Lineage-specific cell lines can be readily obtained from transgenic mice in which the SV40 T-antigen is driven by the expression of a lineage-specific gene such as that of osteocalcin, which is expressed only in osteoblasts and osteocytes (Bonewald, 1999; Kato et al., 1997). MG-63, SaOS-2, U2OS, and HOS cells are available commercially from American Type Culture Collection (Manassas, VA, USA); primary osteoblasts are also purchasable from certain commercial sources. Primary osteoblasts are often derived from marrow aspirates of human trabecular bone after hip or knee arthroplasty or iliac crest bone after spine fusion, or from calvaria of neonatal rats. Human trabecular or iliac crest bone or neonatal rat calvarium is first minced into < 1 mm<sup>3</sup> pieces and then plated in DMEM or  $\alpha$ -MEM culture medium. Cells migrate out from the minced bone fragments and expand to near confluency in about 2-3 weeks. The minced bone pieces can also be digested in

collagenase (1 mg/mL) for 30-60 min or trypsin for  $\leq 15$  min at 37° C prior to plating, to facilitate release of entrapped cells. The osteoblasts should stain positive for alkaline phosphatase, collagen type I, osteocalcin, bone sialoprotein, and calcium phosphate mineral. Osteoprogenitors and multipotent stem cells with osteochondrogenic potential are subpopulations of heterogeneous marrow stromal cells (MSCs) isolated from the medullary cavities of long bones (Peister et al., 2004; Phinney et al., 1999). MSCs are most commonly used to represent osteoprogenitors in experiments involving osteogenic differentiation, as no marker has yet been discovered that specifically identifies and allows purification of pure osteoprogenitors. Human multipotent stem cells capable of differentiating along osteogenic, chondrogenic, and adipogenic lineages are recognized to be positive for CD markers 27, 44, 90, 105, and 166, and negative for hematopoietic markers such as CD34, 45, and 14. Multipotent stem cells can be isolated by flow cytometry with these antibodies, or may be purchased as pre-purified stocks from commercial sources. MSCs are normally isolated from mice by injecting culture medium through surgically dissected femurs and tibias using a 20-25 gauge needle with syringe, and plated directly into culture (Chiu et al., 2006, 2007; Peister et al., 2004; Phinney et al., 1999). Non-adherent blood cells are removed with subsequent medium exchange. The adherent MSCs, which include osteoprogenitor and multipotent stem cells, can be expanded in culture or used immediately for experimentation. MSCs can be induced to undergo osteogenic differentiation in DMEM or  $\alpha$ -MEM containing ascorbic acid or ascorbate-2-phosphate (50  $\mu$ g/mL), dexamethasone (10 nM), and  $\beta$ -glycerophosphate (10 mM) for 2-3 weeks; a series of studies has also included  $1\alpha,25$ -(OH) $_2$ D $_3$  (vitamin D3 or calcitriol, 10 nM) (Wang et al., 2002, 2003). Human MSCs are isolated from femoral medullary canals of total hip arthroplasty patients and plated/expanded in culture in the same fashion (Wang et al., 2002, 2003). The mouse pre-osteoblast cell line, MC3T3-E1, is commonly used to study osteogenic differentiation and its transcriptional mechanisms. Several subclones of MC3T3-E1 exist with different mineralization potentials and expression patterns of osteocalcin and bone sialoprotein (Wang et al., 1999). Mineralizing subclones 4 and 14, and non-mineralizing subclones 24 and 30, of MC3T3-E1 are available from American Type Culture Collection. All subclones of MC3T3-E1 produce collagenous extracellular matrix, are responsive to ascorbic acid, and express alkaline phosphatase and Runx2/Cbfa1 (Choi et al., 1996; Franceschi et al., 1992, 1994; Quarles et al., 1992; Torii et al., 1996; Xiao et al., 1997, 2002).

Osteoblasts, osteoprogenitors, and MSCs are usually treated with particles in 6-, 12-, or 24-well plates, and occasionally in 96-well plates for proliferation and viability assays. Cells are generally plated at an initial density of  $0.5$ - $5.0 \times 10^4$  cells/cm $^2$ , and then treated with particles after 24 hrs of plating or after reaching 70-80% confluency. hMSCs are usually plated at lower cell densities of  $0.5$ - $1.0 \times 10^4$  cells/cm $^2$ , because of their slow proliferation potential and greater difficulty in expanding these cells to large numbers, compared to osteoblast cell lines which proliferate very robustly. Studies have represented particle doses as weight or volume percentages (relative to culture medium volume), number of particles per cell, number of particles per volume of medium, or mass of particles per well or volume of medium. Units can be interconverted based on knowledge of the average diameter of particles, volume of medium per well, and number of cells per well. PMMA and titanium particles are expressed more often as weight or volume percentages (e.g., 0.1, 0.25, 0.50, 1.0% wt), UHMWPE particles are expressed more often as number of particles per mL of medium

( $10^5$ ,  $10^6$ ,  $10^7$ ,  $10^8$  particles/mL), and ceramic particles are at times expressed as mass of particles per volume of medium (e.g., 0.1, 1.0, 10.0 mg/mL). Particle doses are also at times expressed as number of particles per cell (e.g., 5, 50, 500, 5000 particles/cell).

## 7. *In Vivo* experimentation methods

The *in vivo* response of osteoblasts and osteoprogenitors to orthopaedic wear debris has been studied by our group using two systems: the femoral intramedullary injection model and the bone harvest chamber (BHC). These systems have been used extensively to study tissue reactions to wear debris particles in mouse and rabbit systems, and have been important in helping researchers understand the mechanism of wear particle-induced osteolysis, inflammation, and granulomatosis. The femoral intramedullary injection system allows implant particles suspended in saline or hyaluronan carrier solution to be delivered continuously over a period of weeks into the femoral canal of experimental rodents. The system consists of a mini-osmotic Alzet pump (Durect, Cupertino, CA, USA) that is implanted subcutaneously in the dorsal, interscapular region of the animal. The Alzet pump is connected via tubing passed via a surgically created tunnel in the subcutaneous tissue, to a hollow titanium rod 6 mm, 23 gauge in dimensions. The titanium rod is inserted into the femoral medullary canal through a hole drilled in the intercondylar notch (the groove between the femoral condyles) using needles of increasingly larger diameter (e.g., 27, 25, 23, 21, 19 gauge). The pump holds approximately 250  $\mu$ L of particle suspension, usually at a concentration of  $10^9$  to  $10^{10}$  particles/mL, and infuses particles into the femoral canal at a rate of 0.15-0.25  $\mu$ L/hr over several weeks. The titanium rod localizes particles to the marrow canal and prevents their leakage. After several weeks, the tissue reaction to particles can be evaluated by histology, staining for markers of osteoblasts, such as alkaline phosphatase or osteocalcin, and osteoclasts, such as TRAP (tartrate resistant acid phosphatase) or the vitronectin receptor  $\alpha$ V $\beta$ 3 to visualize on microscope for cell number and density. Alternatively, particles can be injected as a single bolus in a suspension volume  $\leq 10$   $\mu$ L, into the tibial medullary canal through a drilled hole in the proximal tibia, as was done in previous studies. The single bolus injection method, however, is less favorable given that it differs from the clinical scenario in which particles are continuously shed from implants over a long period of time; particles injected this way are also not confined as well to the medullary tissue. Local infusion of particles not only allows the study of resident tissue reactions, but also the migratory patterns of luciferase- and GFP-transfected cells injected intravenously into systemic circulation of the animal. Although the femoral intramedullary injection system theoretically allows the behavior of osteoblasts, osteoprogenitors, and multipotent stem cells to be studied *in vivo*, in practice, this rests upon identifying single, specific markers for these cells to facilitate histological identification. Alkaline phosphatase is not specific enough to identify osteoblasts or to distinguish them from osteoprogenitors or pre-osteoblasts. Multipotent stem cells are currently not defined by a single marker, but by a large panel of complex surface markers. The *in vivo* study of osteoblasts, osteoprogenitors, and multipotent stem cells, therefore, rests on the discovery of unique markers that allow for easy and accurate identification of these cells histologically.

The femoral intramedullary injection system involves an arthrotomy of the knee to access the intercondylar notch, which is accomplished via a quadriceps-patellar approach (Zilber et al., 2008). This approach involves a 5-mm incision on the anterior aspect of the knee; the

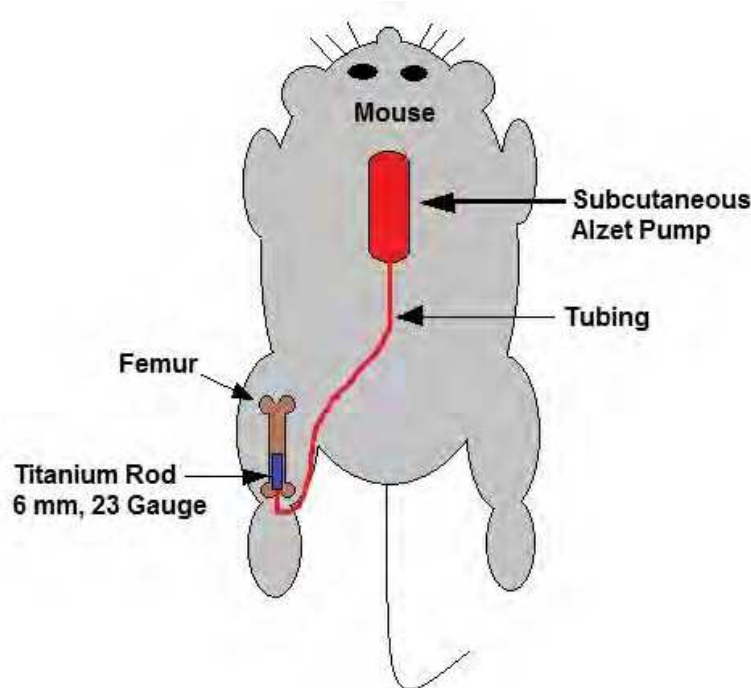


Fig. 3. The femoral intramedullary infusion system (dorsal view of mouse). The model consists of an Alzet mini-osmotic pump that is implanted subcutaneously in the interscapular region of the mouse. The pump is connected via tubing to the titanium rod (6 mm, 23 gauge), which is inserted into the medullary canal of the femur via a hole drilled in the intercondylar notch near the knee joint. The tubing is snugged into a surgically created tunnel in subcutaneous tissue. The pump, which holds about 250  $\mu\text{L}$  of fluid, is used to infuse particle suspensions into the femoral canal at a rate of 0.15-0.25  $\mu\text{L}/\text{hour}$ . This model mimics the clinical situation in which bone and marrow tissue are continuously exposed to wear particles produced from implants.

medial patellar ligament is then incised and the patella laterally displaced, which exposes the intercondylar notch for drilling and subsequent insertion of the titanium rod or particle bolus injection. For particle bolus injection, the traditional quadriceps-patellar or the less invasive transpatellar approach can be used (Zilber et al., 2008). In the transpatellar approach, a similar incision is made on the anterolateral side of the knee, the lateral part of the quadriceps is pushed aside, and without cutting the tendons or ligaments or displacing the patella, the intercondylar notch is directly accessed through the patellar tendon for drilling and particle bolus injection. In both approaches, the needle should be drilled 5 mm into the femoral canal to ensure clear passage through the distal femoral growth plate and to prevent leakage. A study has compared the two approaches in mice and shown successful delivery of 10  $\mu\text{L}$  volumes of 10% PMMA particles into the femoral canal, confirmed subsequently by micro-CT imaging (Zilber et al., 2008).

The efficiency of this *in vivo* particle infusion system has been determined in a series of studies (Ortiz et al., 2008a, 2008b; Ma et al., 2008, 2009a). In this series, the Alzet mini-osmotic pump delivered UHMWPE and polystyrene particles ( $0.5 \pm 0.015 \mu\text{m}$ ) over 4 weeks into an *ex vivo* collection tube. The pump delivered  $10^9$  to  $10^{11}$  particles suspended in 200  $\mu\text{L}$  of mouse serum at a rate of 0.25  $\mu\text{L}/\text{hr}$ . The efficiency of particle delivery was determined by spectrophotometrically measuring the turbidities of the initial and collected outflow

solutions (at 595 nm) and referencing the absorbances against a standard curve of turbidities of known particle concentrations. The efficiency was estimated to be 46% for an original load of  $6 \times 10^9$  polystyrene particles, but it decreased to 23% and then to 15% for approximately each order of magnitude increase in particle number. Efficiency for UHMWPE was approximately one-third for an initial load of  $3 \times 10^{10}$  or  $1.5 \times 10^{11}$  particles (Ortiz et al., 2008a). Particles were successfully pumped into freshly dissected femurs cultured *ex vivo* in DMEM F-12 medium, and were visible in the medullary canal upon gross inspection, particularly with blue-dyed polystyrene particles (Ortiz et al., 2008b). The efficiency of particle delivery has also been evaluated in live mice (Ma et al., 2008, 2009a). Blue-dyed polystyrene particles were injected successfully into the femoral canal of mice over 4 weeks at an efficiency of 40-50% of the initial  $6 \times 10^9$  particles delivered, and were visible on gross inspection of the dissected femurs (Ma et al., 2009a). UHMWPE particles infused into femurs of mice over 4 weeks led to reduced bone volume and higher numbers of macrophages compared to contralateral control femurs with rod but no particles, as assessed by micro-CT and histology/histomorphometry of femoral cross sections (Ma et al., 2008). These studies established the femoral intramedullary injection model as a successful system for delivering particles *in vivo*; improvements however, are needed to increase efficiency of particle delivery.

Another series of studies has used the particle injection method to assess *in vivo* cell responses to titanium particles (Warme et al., 2004; Epstein et al., 2005b; Bragg et al., 2008). In a similar study, UHMWPE particles injected as a single bolus into the femur of C57BL/6 mice (at an average quantity of  $3 \times 10^9$  particles/femur in sodium hyaluronate:PBS carrier solution) also induced intramedullary bone marrow monocytes to increase expression of MCP-1, IL-6, and IL-1 $\beta$  over a 10 week period relative to monocytes from control femurs without particles, as determined by RT-PCR of mRNA from extracted monocytes (Epstein et al., 2005a). In the initial study,  $1.39 \times 10^8$  titanium particles ( $3.7 \pm 1.8 \mu\text{m}$ ) were injected as a single bolus in 10  $\mu\text{L}$  of sodium hyaluronate: PBS carrier solution into the femoral canal, followed by a press-fit 10 mm, 25 gauge stainless steel rod cut from Kirschner wire to prevent particle leakage (Warme et al., 2004). After 26 weeks, femurs were dissected and cultured *ex vivo* in DMEM-F12 for 72 hrs. ELISA analysis of culture media revealed that femurs infused with particles yielded a 45, 79, and 221% increase in production of IL-6, MCP-1, and M-CSF compared to contralateral femurs not infused with particles, whereas IL-1 $\beta$  and TNF- $\alpha$  levels were not elevated (Warme et al., 2004). Histology of femoral cross sections revealed evidence of endosteal bone scalloping and destruction. In a similar study, the same bolus of titanium particles was injected into femurs of knockout mice lacking IL-1r1, the receptor for IL-1 (B6.129s7-Il1r1, Jackson Laboratories, Bar Harbor, ME, USA) (Epstein et al., 2005b). After 20 weeks, femurs were dissected and placed in organ culture. ELISA analysis of culture medium revealed that the production of MCP-1 by femurs infused with particles in these IL-1r1 knockout mice was no different than contralateral control femurs not infused with particles; the absolute levels of MCP-1 production from these experimental femurs were also significantly lower (6-8 fold lower) than those of wild type mice. However, inflammation and bone loss occurred to similar degrees in both IL-1r1 knockout and wild type mice, which indicated that while lack of the IL-1 receptor limited MCP-1 production, it did not abolish or reduce the overall inflammatory response to particles, due perhaps to activation of alternative inflammatory pathways (Epstein et al., 2005b). A followup study demonstrated histological evidence of inflammation and

endosteal erosion characterized by fibrosis, jagged cortical margins, increased porosity, and presence of a periprosthetic membrane in femoral canals of IL-1r1 knockout mice injected with a bolus of titanium particles (Bragg et al., 2008).

The particle injection method has also been employed to study migratory patterns of injected cells, which may theoretically be extended to luciferase- and GFP-labeled marrow stromal or multipotent stem cells, osteoprogenitors, and osteoblasts. A series of studies has tracked the systemic migration of luciferase-transfected reporter macrophages injected into the lateral tail vein of nude mice with previous injection or infusion of particles into the femur (Ren et al., 2008, 2010, 2011). In one study, Simplex P bone cement powder 1-100  $\mu\text{m}$  in diameter (Howmedica Osteonics, Allendale, NJ, USA) consisting of 15% PMMA, 75% methylmethacrylate styrene copolymer, and 10% barium sulfate, as a 10% wt suspension in PBS, was injected as a single bolus of 10  $\mu\text{L}$  into the femoral canal of nude mice, followed 7 days later by injection of luciferase- and GFP-transfected Raw264.7 macrophages ( $5 \times 10^5$  cells in 100  $\mu\text{L}$  HBSS) into their lateral tail vein (Ren et al., 2008). Bioluminescence imaging of mice revealed significantly higher bioluminescent signal in particle-infused femurs at days 6 and 8 post-macrophage injection ( $4.7 \pm 1.6$ ,  $7.8 \pm 2.9$  respectively, ratios of signal of particle-infused femur over contralateral control femur), compared to those of saline-injected controls ( $1.2 \pm 0.2$ ,  $1.4 \pm 0.5$ ). Histological analysis of femoral cross sections also showed higher numbers of GFP- and MOMA-2-positive macrophages (MOMA-2 is a macrophage marker) in the particle-infused femurs than in control femurs. The imaging and histology results indicated that macrophages from systemic sites migrated to tissues injured by wear debris particles. Similarly, UHMWPE particles ( $1.0 \pm 0.1 \mu\text{m}$ ) injected as a single bolus of  $1.2 \times 10^8$  particles in 10  $\mu\text{L}$  into femora of nude mice attract luciferase- and GFP-transfected Raw264.7 macrophages to its site of infusion, resulting in significantly larger bioluminescent signals ( $10.32 \pm 7.61$  signal ratio) than saline-injected control femurs (signal ratio close to 1) 8 days after macrophage injection. Histological analysis revealed larger number of Raw264.7 macrophages positive for GFP and  $\alpha\text{V}\beta 3$ -positive osteoclasts in particle-infused femurs compared to saline-injected control femurs (Ren et al., 2010). UHMWPE particles continuously infused into femora of nude mice by the Alzet mini-osmotic pump (rather than by single bolus injection), also attracted labeled Raw264.7 macrophages to their site of infusion (Ren et al., 2011). Ten days after macrophage injection, femurs extracted for histology demonstrated increased numbers of GFP-labeled Raw264.7 macrophages, total macrophages (MOMA-2-positive), and vitronectin receptor/TRAP-positive osteoclasts in particle-infused samples than in saline-treated control femurs. Some cells stained positive for both TRAP and MOMA-2, and represent monocytes that have differentiated into osteoclasts. Bioluminescence imaging revealed significantly higher signal ratios in particle-infused femurs ( $13.95 \pm 5.65$ ) compared to saline-treated femurs with signal ratios close to 1. MicroCT scans of femurs infused with particles revealed decreased bone mineral density compared to saline-infused femurs (Ren et al., 2011). Taken together, these results indicate that systemic macrophages migrate to sites of particle infusion in response to particle-induced inflammation. The same model can potentially be applied to study the migratory patterns of systemically infused marrow stromal or multipotent stem cells, osteoprogenitors, and osteoblasts, which may respond to secreted cues of bone injury or osteolysis. The applicability of this model for this purpose rests upon identifying markers that allow appropriate isolation of pure osteogenic cell and progenitor populations for labeling with luciferase or fluorescent proteins.

In vivo cell responses to orthopaedic wear debris can also be evaluated using the bone harvest chamber (BHC). A modified version of the BHC, the drug test chamber (DTC), also allows evaluation of cell responses to infused therapeutic agents and growth factors in vivo under simultaneous exposure to wear particles. Earlier studies on in vivo tissue responses have been conducted by direct surgical implantation of particle boluses (e.g., 60-70 mg of PMMA cement powder) into the medullary tibial canal of rabbits via a drilled hole in the proximal tibia (Goodman et al., 1988, 1991a, 1991b). Though these studies have helped to elucidate the response of tissues to wear debris particles, the introduction of the BHC in the early 1990s has greatly facilitated this research process (Goodman et al., 1994, 1995a, 1995b, 1995c, 1996a, 1996b). The BHC is a titanium device with an inner core containing a  $1 \times 1 \times 5$  mm<sup>3</sup> pathway for tissue ingrowth and an outer cylindrical shell with threads for screwing the cylinder into the surrounding bone. The outer shell contains  $1 \times 1$  mm<sup>2</sup> openings on its two ends that are continuous with the pathway in the inner chamber. When implanted into bone, the BHC allows bone ingrowth into its inner core; this bone tissue specimen can be collected at multiple times by removing the inner core, without disrupting the outer shell that has integrated with surrounding bone. In addition, particle suspensions can be placed inside the inner pathway such that ingrown bone reacts to these particulates, allowing the tissue reaction to be studied by histology after retrieval of the tissue sample. The DTC is essentially the BHC setup with an additional Alzet mini-osmotic pump that allows biologics to be infused into the inner core at a regulated rate. This mimics the clinical scenario in which therapeutic drugs are delivered locally to an area of tissue ingrowth. The DTC contains a 10  $\mu$ L reservoir for holding the infused solution and is linked to the inner core for bone ingrowth. The Alzet pump, which contains around 250  $\mu$ L of solution, is implanted subcutaneously in the animal and infuses fluid at a rate of 0.25  $\mu$ L/hr to the DTC reservoir via tubing. From there, the fluid travels to the inner chamber where the tissue is ingrowing and exposed to particles. As fluid builds up in the inner chamber, it is drained via outlet tubing to the skin of the animal. The Alzet pump and its tubing can also be removed and replaced with minimal disturbance to the system. The size of the BHC/DTC permits this device to be used only for rabbits or larger animals. With appropriate markers to identify multipotent stem cells, osteoprogenitors, and osteoblasts, the in vivo behavior of these cells in response to wear particles can potentially be studied using the harvest chamber models.

The BHC has been used in a series of studies to evaluate in vivo tissue responses to wear particles during administration of oral p38 MAP kinase inhibitors in rabbits (Goodman et al., 2007; Ma et al., 2009). p38 MAP kinase mediates various pathways in inflammation, apoptosis, and osteoclast differentiation. In one study, BHCs were implanted and allowed to osseointegrate into the proximal tibial metaphyses of rabbits for 6 weeks. Ingrown tissue was removed and replaced with UHMWPE particles ( $0.5 \pm 0.2$   $\mu$ m) at a concentration of  $7.5 \times 10^9$  particles in 5  $\mu$ L in 1% sodium hyaluronate carrier solution at one of the 3-week treatment time intervals, with or without oral administration of p38 MAPK inhibitor, with comparison to control BHCs filled with carrier solution only. Tissue ingrowth into the BHC chamber was collected at the end of 3 weeks, and assessed histologically for expression of alkaline phosphatase (osteoblasts) or vitronectin receptor (osteoclasts) (Goodman et al., 2007). Histology tissue sections were also histomorphometrically quantified, using NIH Imaging software, for total tissue area, total bone area, ratio of total bone area over total tissue area, and total area of alkaline phosphatase-positive stains, and counted for the number of vitronectin receptor-positive cells. The oral p38 MAPK inhibitor, expected to

inhibit inflammation and bone loss, actually yielded diminished bone ingrowth and alkaline phosphatase staining, and failed to suppress inflammation or foreign body reactions in the presence of UHMWPE particles (Goodman et al., 2007). A later study testing the effects of the oral p38 MAPK inhibitor SCIO-323, has shown similar results of reduced bone growth with no curtailment of inflammation in particle-treated groups, compared to particle-treated controls not receiving SCIO-323 (Ma et al., 2009). In summary, the BHC experiments have shown that p38 MAPK inhibitors do not improve bone formation in tissues exposed to wear debris particles.

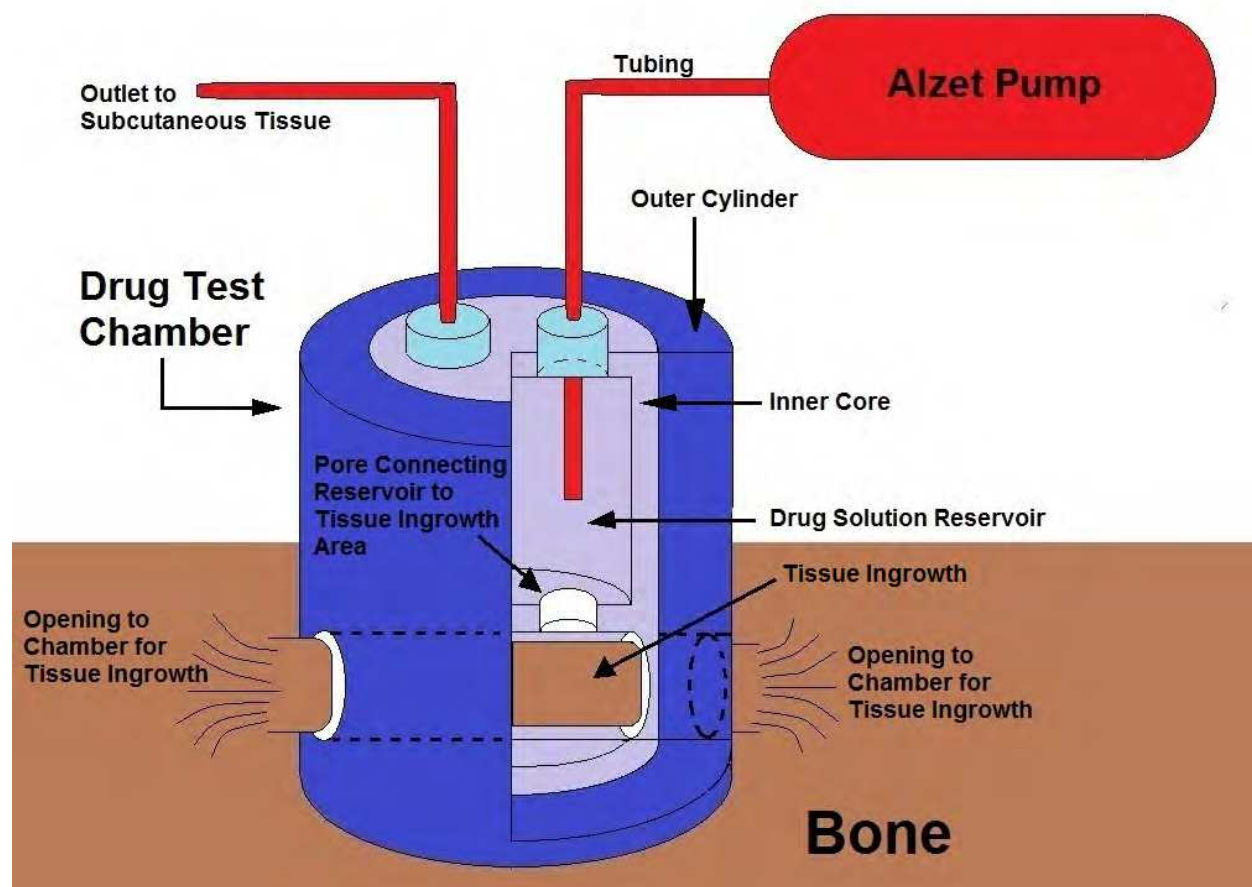


Fig. 4. The drug test chamber (DTC). This system consists of a titanium chamber that permits tissue ingrowth, and an Alzet mini-osmotic pump for infusing biologics into the chamber. The titanium chamber consists of an outer cylinder that allows the device to be screwed into surrounding bone, and an inner core composed of a 10  $\mu$ L reservoir for holding infused solution and an inner canal/pathway for tissue ingrowth. The inner core is separable from the outer cylinder and allows the ingrown tissue to be collected without disrupting the entire device. The Alzet pump infuses solutions into the reservoir of the inner core, which in turn is connected to the tissue ingrowth canal via an open pore. Fluid outflow is drained via tubing to the subcutaneous tissue.

The DTC has been employed in a series of studies to evaluate *in vivo* tissue responses to wear particles during local infusion of trophic, osteogenic, or anti-inflammatory factors (Goodman et al., 2003a, 2003b; Ma et al., 2006). In one study, DTC was used to infuse FGF-2,

a growth factor that modulates osteoblast proliferation, differentiation, bone formation, and angiogenesis, in the presence of UHMWPE particles in rabbits (Goodman et al., 2003a). FGF-2 was infused at a dose of 50 ng/day over 3 weeks into the DTC, in the presence of a low ( $5.8 \times 10^{11}$  particles/mL) or high ( $1.7 \times 10^{12}$  particles/mL) concentration of UHMWPE particles ( $0.5 \pm 0.2 \mu\text{m}$ ). After 3 weeks, tissues extracted for histology and histomorphometric analysis revealed that FGF-2 significantly increased bone growth and decreased the number of vitronectin receptor-positive osteoclasts in samples treated with UHMWPE particles, compared to particle-treated samples not infused with FGF-2 (Goodman et al., 2003a). In another study, the DTC was infused with IL-10, an anti-inflammatory cytokine that suppresses Th1 helper cell-mediated inflammation, including expression of IL-1, IL-6, IL-8, TNF- $\alpha$ , and GM-CSF, in the presence of UHMWPE particles in rabbits (Goodman et al., 2003b). IL-10 was infused at increasing doses of 0.1, 1.0, 10.0 and 100.0 ng/mL for 3 weeks at each dose, in the presence or absence of UHMWPE particles ( $1.7 \times 10^{12}$  particles/mL) in the DTC. Histology and histomorphometric analysis revealed that IL-10 infused at 1.0 ng/mL for 3 weeks, significantly increased bone growth up to 48% in the presence of UHMWPE particles, compared to particle-treated samples without IL-10. In the absence of particles, IL-10 had no effect on bone growth relative to controls not treated with IL-10 (Goodman et al., 2003b). In another study, the DTC was infused with OP-1 (also called BMP-7), a growth factor that promotes osteoblast proliferation, differentiation, and mineralization, in the presence of UHMWPE particles in rabbits (Ma et al., 2006). Infusion of OP-1 (110 ng/day) into the DTC for 6 weeks increased bone growth by 38% in the presence of UHMWPE particles, relative to particle-treated samples without OP-1 (Ma et al., 2006).

## 8. References

- [1] Abbas S, Clohisy JC, Abu-Amer Y. (2003). Mitogen-activated protein (MAP) kinases mediate PMMA-induction of osteoclasts. *J Orthop Res*, Vol. 21, No. 6, pp. 1041-1048.
- [2] Affatato S, Fernandes B, Tucci A, Esposito L, Toni A. (2001). Isolation and morphological characterization of UHMWPE wear debris generated in vitro. *Biomaterials*, Vol. 22, No. 17, pp. 2325-2331.
- [3] Allen MJ, Myer BJ, Millett PJ, Rushton N. (1997). The effects of particulate cobalt, chromium and cobalt-chromium alloy on human osteoblast-like cells in vitro. *J Bone Joint Surg Br*, Vol. 79, No. 3, pp. 475-482.
- [4] Andrews RE, Shah KM, Wilkinson JM, Gartland A. (2011). Effects of cobalt and chromium ions at clinically equivalent concentrations after metal-on-metal hip replacement on human osteoblasts and osteoclasts: implications for skeletal health. *Bone*, Vol. 49, No. 4, pp. 717-723.
- [5] Atkins GJ, Welldon KJ, Holding CA, Haynes DR, Howie DW, Findlay DM. (2009). The induction of a catabolic phenotype in human primary osteoblasts and osteocytes by polyethylene particles. *Biomaterials*, Vol. 30, No. 22, pp. 3672-3681.
- [6] Bi Y, Collier TO, Goldberg VM, Anderson JM, Greenfield EM. (2002). Adherent endotoxin mediates biological responses of titanium particles without stimulating their phagocytosis. *J Orthop Res*, Vol. 20, No. 4, pp. 696-703.
- [7] Bi Y, Seabold JM, Kaar SG, Ragab AA, Goldberg VM, Anderson JM, Greenfield EM. (2001). Adherent endotoxin on orthopedic wear particles stimulates cytokine

- production and osteoclast differentiation. *J Bone Miner Res*, Vol. 16, No. 11, pp. 2082-2091.
- [8] Bonewald LF. (1999). Establishment and characterization of an osteocyte-like cell line, MLO-Y4. *J Bone Miner Metab*, Vol. 17, No. 1, pp. 61-65.
- [9] Bragg B, Epstein N, Ma T, Goodman S, Smith RL. (2008). Histomorphometric analysis of the intramedullary bone response to titanium particles in wild-type and IL-1R1 knock-out mice: a preliminary study. *J Biomed Mater Res B Appl Biomater*, Vol. 84, No. 2, pp. 559-570.
- [10] Campbell P, Ma S, Yeom B, McKellop H, Schmalzried TP, Amstutz HC. (1995). Isolation of predominantly submicron-sized UHMWPE wear particles from periprosthetic tissues. *J Biomed Mater Res*, Vol. 29, No. 1, pp. 127-131.
- [11] Chiu R, Ma T, Smith RL, Goodman SB. (2006). Polymethylmethacrylate particles inhibit osteoblastic differentiation of bone marrow osteoprogenitor cells. *J Biomed Mater Res A*, Vol. 15, No. 4, pp. 850-856.
- [12] Chiu R, Ma T, Smith RL, Goodman SB. (2007). Kinetics of polymethylmethacrylate particle-induced inhibition of osteoprogenitor differentiation and proliferation. *J Orthop Res*, Vol. 25, No. 4, pp. 450-457.
- [13] Chiu R, Ma T, Smith RL, Goodman SB. (2008). Polymethylmethacrylate particles inhibit osteoblastic differentiation of MC3T3-E1 osteoprogenitor cells. *J Orthop Res*, Vol. 26, No. 7, pp. 932-936.
- [14] Chiu R, Ma T, Smith RL, Goodman SB. (2009). Ultrahigh molecular weight polyethylene wear debris inhibits osteoprogenitor proliferation and differentiation in vitro. *J Biomed Mater Res A*, Vol. 89, No. 5, pp. 242-247.
- [15] Chiu R, Smith KE, Ma GK, Ma T, Smith RL, Goodman SB. (2010). Polymethylmethacrylate particles impair osteoprogenitor viability and expression of osteogenic transcription factors Runx2, osterix, and Dlx5. *J Orthop Res*, Vol. 28, No. 5, pp. 571-577.
- [16] Chiu R, Smith RL, Goodman SB. (2010). Polymethylmethacrylate particles inhibit human mesenchymal stem cell osteogenesis, *Proceedings of Society for Biomaterials*, Seattle, April 2010.
- [17] Choi JY, Lee BH, Song KB, Park RW, Kim IS, Sohn KY, Jo JS, Ryoo HM. (1996). Expression patterns of bone-related proteins during osteoblastic differentiation in MC3T3-E1 cells. *J Cell Biochem*, Vol. 61, No. 4, pp. 609-618.
- [18] Choi MG, Koh HS, Kleuss D, O'Connor D, Mathur A, Truskey GA, Rubin J, Zhou DX, Sung KL. (2005). Effects of titanium particle size on osteoblast functions in vitro and in vivo. *Proc Natl Acad Sci USA*, Vol. 102, No. 12, pp. 4578-4583.
- [19] Ciapetti G, Gonzales-Carrasco JL, Savarino L, Montealegre MA, Pagani S, Baldini N. (2005). Quantitative assessment of the response of osteoblast- and macrophage-like cells to particles of Ni-free Fe-base alloys. *Biomaterials*, Vol. 26, No. 8, pp. 849-859.
- [20] Clohisy JC, Yamanak Y, Faccio R, Abu-Amer Y. (2006). Inhibition of IKK activation, through sequestering NEMO, blocks PMMA-induced osteoclastogenesis and calvarial inflammatory osteolysis. *J Orthop Res*, Vol. 24, No. 7, pp. 1358-1365.
- [21] Dean DD, Lohmann CH, Sylvia VL, Koster G, Liu Y, Schwartz Z, Boyan BD. (2001). Effect of polymer molecular weight and addition of calcium stearate on response of MG63 osteoblast-like cells to UHMWPE particles. *J Orthop Res*, Vol. 19, No. 2, pp. 179-86.

- [22] Dean DD, Schwartz Z, Blanchard CR, Liu Y, Agrawal CM, Lohmann CH, Sylvia VL, Boyan BD. (1999). Ultrahigh molecular weight polyethylene particles have direct effects on proliferation, differentiation, and local factor production of MG63 osteoblast-like cells. *J Orthop Res*, Vol. 17, No. 1, pp. 9-17.
- [23] Dean DD, Schwartz Z, Liu Y, Blanchard CR, Agrawal CM, Mabrey JD, Sylvia VL, Lohmann CH, Boyan BD. (1999). The effect of ultra-high molecular weight polyethylene wear debris on MG63 osteosarcoma cells in vitro. *J Bone Joint Surg Am*, Vol. 81, No. 4, pp. 452-461.
- [24] DeLaSalle H, Benghuzzi H, Deville R, Tucci M. (2006). The effects of PMMA particle number on MG-63 osteoblast cell function. *Biomed Sci Instrum*, Vol. 42, 48-53.
- [25] Epstein NJ, Bragg WE, Ma T, Spanogle J, Smith RL, Goodman SB. (2005). UHMWPE wear debris upregulates mononuclear cell proinflammatory gene expression in a novel murine model of intramedullary particle disease. *Acta Orthop*, Vol. 76, No. 3, pp. 412-420.
- [26] Epstein NJ, Warme BA, Spanogle J, Ma T, Bragg B, Smith RL, Goodman SB. (2005). Interleukin-1 modulates periprosthetic tissue formation in an intramedullary model of particle-induced inflammation. *J Orthop Res*, Vol. 23, No. 3, pp. 501-510.
- [27] Fleury C, Petit A, Antoniou J, Zukor DJ, Tabrizian M, Huk OL. (2006). Effect of cobalt and chromium ions on human MG-63 osteoblasts in vitro: morphology, cytotoxicity, and oxidative stress. *Biomaterials*, Vol. 27, No., 18, pp. 3351-3360.
- [28] Franceschi RT, Bhanumathi SI, Cui Y. (1994). Effects of ascorbic acid on collagen matrix formation and osteoblast differentiation in murine MC3T3-E1 cells. *J Bone Miner Res*, Vol. 9, No. 6, pp. 843-854.
- [29] Franceschi RT, Iyer BS. (1992). Relationship between collagen synthesis and expression of the osteoblast phenotype in MC3T3-E1 cells. *J Bone Miner Res*, Vol. 7, No. 2, pp. 235-246.
- [30] Fritz EA, Glant TT, Vermes C, Jacobs JJ, Roebuck KA. (2002). Titanium particles induce the immediate early stress responsive chemokines IL-8 and MCP-1 in osteoblasts. *J Orthop Res*, Vol. 20, No. 3, pp. 490-498.
- [31] Fritz EA, Glant TT, Vermes C, Jacobs JJ, Roebuck KA. (2006). Chemokine gene activation in human bone marrow-derived osteoblasts following exposure to particulate wear debris. *J Biomed Mater Res A*, Vol. 77, No. 1, pp. 192-201.
- [32] Fritz EA, Jacobs JJ, Glant TT, Roebuck KA. (2005). Chemokine IL-8 induction by particulate wear debris in osteoblasts is mediated by NF-kappaB. *J Orthop Res*, Vol. 23, No. 6, pp. 1249-1257.
- [33] Goodman S, Aspenberg P, Song Y, Doshi A, Regula D, Lidgren L. (1995). Effects of particulate high-density polyethylene and titanium alloy on tissue ingrowth into bone harvest chamber in rabbits. *J Appl Biomater*, Vol. 6, No. 1, pp. 27-33.
- [34] Goodman S, Aspenberg P, Song Y, Knoblich G, Huie P, Regula D, Lidgren L. (1995). Tissue ingrowth and differentiation in the bone-harvest chamber in the presence of cobalt-chromium-alloy and high-density-polyethylene particles. *J Bone Joint Surg Am*, Vol. 77, No. 7, pp. 1025-1035.
- [35] Goodman S, Aspenberg P, Song Y, Regula D, Lidgren L. (1995). Intermittent micromotion and polyethylene particles inhibit bone ingrowth into titanium chambers in rabbits. *J Appl Biomater*, Vol. 6, No. 3, pp. 161-165.

- [36] Goodman S, Aspenberg P, Song Y, Regula D, Lidgren L. (1996). Polyethylene and titanium alloy particles reduce bone formation. *Acta Orthop Scand*, Vol. 67, No. 6, pp. 599-605.
- [37] Goodman S, Trindade, Ma T, Lee M, Wang N, Ikenou T, Matsuura I, Miyanishi K, Fox N, Regula D, Genovese G, Klein J, Bloch D, Smith RL. (2003). Modulation of bone ingrowth and tissue differentiation by local infusion of interleukin-10 in presence of ultra-high molecular weight polyethylene (UHMWPE) wear particles. *J Biomed Mater Res A*, Vol. 65, No. 1, pp. 43-50.
- [38] Goodman SB, Chin RC, Chiou SS, Lee JS. (1991). Suppression of prostaglandin E2 synthesis in the membrane surrounding particulate polymethylmethacrylate in the rabbit tibia. *Clin Orthop Relat Res*, Vol. 271, pp. 300-304.
- [39] Goodman SB, Davidson JA, Song Y, Martial N, Fornasier VL. (1996). Histomorphological reaction of bone to different concentrations of phagocytosable particles of high-density polyethylene and Ti-6Al-4V alloy in vivo. *Biomaterials*, Vol. 17, No. 20, pp. 1943-1947.
- [40] Goodman SB, Fornasier VL, Kei J. (1988). The effects of bulk versus particulate polymethylmethacrylate on bone. *Clin Orthop Relat Res*, Vol. 232, pp. 255-262.
- [41] Goodman SB, Fornasier VL, Kei J. (1991). Quantitative comparison of the histological effects of particulate polymethylmethacrylate versus polyethylene in rabbit tibia. *Arch Orthop Trauma Surg*, Vol. 110, No. 3, pp. 123-126.
- [42] Goodman SB, Ma T, Spanogle J, Chiu R, Miyanishi K, Oh K, Plouhar P, Wadsworth S, Smith RL. (2007). Effects of a p38 MAP kinase inhibitor on bone ingrowth and tissue differentiation in rabbit chambers. *J Biomed Mater Res A*, Vol. 81, No. 2, pp. 310-316.
- [43] Goodman SB, Song Y, Yoo JY, Fox N, Trindade MC, Kajiyama G, Ma T, Regular D, Brown J, Smith RL. (2003). Local infusion of FGF-2 enhances bone ingrowth in rabbit chambers in presence of polyethylene particles. *J Biomed Mater Res A*, Vol. 65, No. 4, pp. 454-461.
- [44] Goodman SB. (1994). The effects of micromotion and particulate materials on tissue differentiation: bone chamber studies in rabbits. *Acta Orthop Scand Suppl*, Vol. 258, pp. 1-43.
- [45] Granchi D, Amato I, Battistelli L, Ciapetti G, Pagani S, Avnet S, Baldini N, Giunti A. (2005). Molecular basis of osteoclastogenesis induced by osteoblasts exposed to wear particles. *Biomaterials*, Vol. 26, No. 15, pp. 237-239.
- [46] Granchi D, Ciapetti G, Amato I, Pagani S, Cenni E, Savarino L, Avnet S, Peris JL, Pallacani A, Baldini N, Giunti A. (2004). The influence of alumina and ultra-high molecular weight polyethylene particles on osteoblast-osteoclast cooperation. *Biomaterials*, Vol. 25, No. 18, pp. 4037-45.
- [47] Greenfield EM, Bechtold J, Implant Wear Symposium 2007 Biologic Work Group. (2008). What other biologic and mechanical factors might contribute to osteolysis? *J Am Acad Orthop Surg*, Vol. 16, Suppl 1, pp. S56-62.
- [48] Greenfield EM, Bi Y, Ragab AA, Goldberg VM, Nalepka JL, Seabold JM. (2005). Does endotoxin contribute to aseptic loosening of orthopedic implants? *J Biomed Mater Res B Appl Biomater*, Vol. 72, No. 1, pp. 179-185.

- [49] Gregory CA, Gunn WG, Peister A, Prockop DJ. (2004). An Alizarin red-based assay of mineralization by adherent cells in culture: comparison with cetylpyridinium chloride extraction. *Anal Biochem*, Vol. 329, No. 1, pp. 77-84.
- [50] Heinemann DE, Lohmann C, Siggelkow H, Alves F, Engel I, Koster G. (2000). Human osteoblast-like cells phagocytose metal particles and express the macrophage marker CD68 in vitro. *J Bone Joint Surg Br*, Vol. 82, No. 2, pp. 283-289.
- [51] Jeong WK, Park SW, Im GI. (2008). Growth factors reduce the suppression of proliferation and osteogenic differentiation by titanium particles on MSCs. *J Biomed Mater Res A*, Vol. 86, No. 4, pp. 1137-1144.
- [52] Kanaji A, Caicedo MS, Viridi AS, Sumner DR, Hallab NJ, Sena K. (2009). Co-Cr-Mo alloy particles induce tumor necrosis factor alpha production in MLO-Y4 osteocytes: a role for osteocytes in particle-induced inflammation. *Bone*, Vol. 45, No. 3, pp. 528-533.
- [53] Kann S, Chiu R, Ma T, Goodman SB. (2010). OP-1 (BMP-7) stimulates osteoprogenitor cell differentiation in the presence of polymethylmethacrylate particles. *J Biomed Mater Res A*, Vol. 94, No. 2, pp. 485-488.
- [54] Kato Y, Windle JJ, Koop BA, Mundy GR, Bonewald LF. (1997). Establishment of an osteocyte-like cell line, MLO-Y4. *J Bone Miner Res*, Vol. 12, No. 12, pp. 2014-2023.
- [55] Komori T. (2006). Regulation of osteoblast differentiation by transcription factors. *J Cell Biochem*, Vol. 99, No. 5, pp. 1233-1239.
- [56] Kurtz SM. (2004). *The UHMWPE Handbook: Ultra-High Molecular Weight Polyethylene in Total Joint Replacement*, Academic Press, ISBN 0-12-429851-6, San Diego, United States of America.
- [57] Kwon SY, Lin T, Takei H, Ma Q, Wood DJ, O'Connor D, Sung KL. (2001). Alterations in the adhesion behavior of osteoblasts by titanium particle loading: inhibition of cell function and gene expression. *Biorheology*, Vol. 38, No. 2-3, pp. 161-83.
- [58] Kwon SY, Takei H, Pioletti DP, Lin T, Ma QJ, Akeson WH, Wood DJ, Sung KL. (2000). Titanium particles inhibit osteoblast adhesion to fibronectin-coated substrates. *J Orthop Res*, Vol. 18, No. 2, pp. 203-211.
- [59] Lenz R, Mittelmeier W, Hansmann D, Brem R, Diehl P, Fritsche A, Bader R. (2009). Response of human osteoblasts exposed to wear particles generated at the interface of total hip stems and bone cement. *J Biomed Mater Res A*, Vol. 89, No. 2, pp. 370-378.
- [60] Lian JB, Stein GS. (2001). Osteoblast biology. In: *Osteoporosis, 2nd ed.*, Marcus R, Feldman D, Kelsey J. pp. 21-71, Academic Press, ISBN 978-0-12-470862-4, San Diego, United States of America.
- [61] Liu F, Zhu Z, Mao Y, Liu M, Tang T, Qiu S. (2009). Inhibition of titanium particle-induced osteoclastogenesis through inactivation of NFATc1 by VIVIT peptide. *Biomaterials*, Vol. 30, No. 9, pp. 1756-1762.
- [62] Lohmann CH, Dean DD, Bonewald LF, Schwartz Z, Boyan BD. (2002). Nitric oxide and prostaglandin E2 production in response to ultra-high molecular weight polyethylene particles depends on osteoblast maturation state. *J Bone Joint Surg Am*, Vol. 84, No. 3, pp. 411-419.
- [63] Lohmann CH, Dean DD, Koster G, Casasola D, Buchhorn GH, Fink U, Schwartz Z, Boyan BD. (2002). Ceramic and PMMA particles differentially affect osteoblast phenotype. *Biomaterials*, Vol. 23, No. 8, pp. 1855-1863.

- [64] Lohmann CH, Schwartz Z, Koster G, Jahn U, Buchhorn GH, MacDougall MJ, Casasola D, Liu Y, Sylvia VL, Dean DD, Boyan BD. (2000). Phagocytosis of wear debris by osteoblasts affects differentiation and local factor production in a manner dependent on particle composition. *Biomaterials*, Vol. 21, No. 6, pp. 551-561.
- [65] Ma G, Chiu R, Huang Z, Pearl K, Ma T, Smith RL, Goodman SB. (2010). Polymethylmethacrylate particle exposure causes changes in p38 MAPK and TGF-beta signalling in differentiating MC3T3-E1 cells. *J Biomed Mater Res A*, Vol. 94, No. 1, pp. 234-240.
- [66] Ma T, Huang Z, Ren PG, McCally R, Lindsey D, Smith RL, Goodman SB. (2008). An in vivo murine model of continuous intramedullary infusion of particles. *Biomaterials*, Vol. 29, No. 27, pp. 3738-3742.
- [67] Ma T, Nelson ER, Mawatari T, Oh KJ, Larsen DM, Smith RL, Goodman SB. (2006). Effects of local infusion of OP-1 on particle-induced and NSAID-induced inhibition of bone ingrowth in vivo. *J Biomed Mater Res A*, Vol. 79, No. 3, pp. 740-746.
- [68] Ma T, Ortiz SG, Huang Z, Ren PG, Smith RL, Goodman SB. (2009). In vivo murine model of continuous intramedullary infusion of particles: a preliminary study. *J Biomed Mater Res B Appl Biomater*, Vol. 88, No.1, pp. 250-253.
- [69] Ma T, Ren PG, Larsen DM, Suenaga E, Zilber S, Genovese M, Smith RL, Goodman SB. (2009). Efficacy of a p38 mitogen activated protein kinase inhibitor in mitigating an established inflammatory reaction to polyethylene particles in vivo. *J Biomed Mater Res A*, Vol. 89, No. 1, pp. 117-123.
- [70] Malaval L, Liu F, Roche P, Aubin JE. (1999). Kinetics of osteoprogenitor proliferation and osteoblast differentiation in vitro. *J Cell Biochem*, Vol. 74, No. 4, pp. 616-627.
- [71] Maloney WJ, Smith RL, Schmalzried TP, Chiba J, Huene D, Rubash H. (1995). Isolation and characterization of wear particles generated in patients who have had failure of a hip arthroplasty without cement. *J Bone Joint Surg Am*, Vol. 77, No. 9, pp. 1301-1310.
- [72] Martinez ME, Medina S, del Campo MT, Garcia JA, Rodrigo A, Munuera L. (1998). Effect of polyethylene particles on human osteoblastic cell growth. *Biomaterials*, Vol. 19, No. 1-3, pp. 183-187.
- [73] Martinez ME, Medina S, del Campo MT, Sanchez-Cabezudo MJ, Sanchez M, Munuera L. (1998). Effect of polyethylene on osteocalcin, alkaline phosphatase, and procollagen secretion by human osteoblastic cells. *Calcif Tissue Int*, Vol. 62, No. 5, pp. 453-456.
- [74] Minoda Y, Kobayashi A, Iwaki H, Miyaguchi M, Kadoya Y, Ohashi H, Takaoka K. (2004). Characteristics of polyethylene wear particles isolated from synovial fluid after mobile-bearing and posterior-stabilized total knee arthroplasties. *J Biomed Mater Res B Appl Biomater*, Vol. 71, No. 1, pp. 1-6.
- [75] Nalepka JL, Lee MJ, Kraay MJ, Marcus RE, Goldberg VM, Chen X, Greenfield EM. (2006). Lipopolysaccharide found in aseptic loosening of patients with inflammatory arthritis. *Clin Orthop Relat Res*, Vol. 451, pp. 229-235.
- [76] O'Connor DT, Choi MG, Kwon SY, Paul Sung KL. (2004). New insight into the mechanism of hip prosthesis loosening: effect of titanium debris size on osteoblast function. *J Orthop Res*, Vol. 22, No. 2, pp. 229-236.

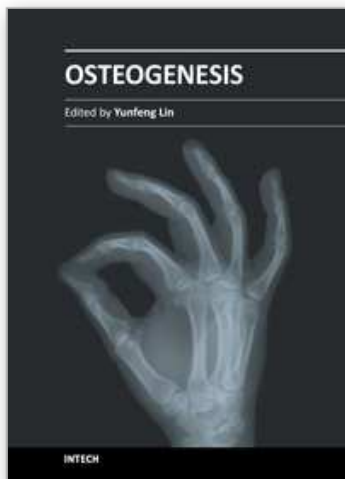
- [77] Okafor CC, Haleem-Smith H, Laqueriere P, Manner PA, Tuan RS. (2006). Particulate endocytosis mediates biological responses of human mesenchymal stem cells to titanium wear debris. *J Orthop Res*, Vol. 24, No. 3, pp. 461-473.
- [78] Ortiz SG, Ma T, Epstein NJ, Smith RL, Goodman SB. (2008). Validation and quantification of an in vitro model of continuous infusion of submicron-sized particles. *J Biomed Mater Res B Appl Biomater*, Vol. 84, No. 2, pp. 328-333.
- [79] Ortiz SG, Ma T, Regula D, Smith RL, Goodman SB. (2008). Continuous intramedullary polymer particle infusion using a murine femoral explants model. *J Biomed Mater Res B Appl Biomater*, Vol. 87, No. 2, pp. 440-446.
- [80] Peister A, Mellad JA, Larson BL, Hall BM, Gibson LF, Prockop DJ. (2004). Adult stem cells from bone marrow (MSCs) isolated from different strains of inbred mice vary in surface epitopes, rates of proliferation, and differentiation potential. *Blood*, Vol. 103, No. 5, pp. 1662-1668.
- [81] Peter B, Zambelli PY, Guicheux J, Pioletti DP. (2005). The effect of bisphosphonates and titanium particles on osteoblasts: an in vitro study. *J Bone Joint Surg Br*, Vol. 87, No. 8, pp. 1157-63.
- [82] Phinney DG, Kopen G, Isaacson RL, Prockop DJ. (1999). Plastic adherent stromal cells from the bone marrow of commonly used strains of inbred mice: variations in yield, growth, and differentiation. *J Cell Biochem*, Vol. 72, No. 4, pp. 570-585.
- [83] Pioletti DP, Leoni L, Genini D, Takei H, Du P, Corbeil J. (2002). Gene expression analysis of osteoblastic cells contacted by orthopedic implant particles. *J Biomed Mater Res*, Vol. 61, No. 3, pp. 408-20.
- [84] Piolett DP, Kottelat A. (2004). The influence of wear particles in the expression of osteoclastogenesis factors by osteoblasts. *Biomaterials*, Vol. 25, No. 27, pp. 5803-5808.
- [85] Pioletti DP, Takei H, Kwon SY, Wood D, Sung KL. (1999). The cytotoxic effect of titanium particles phagocytosed by osteoblasts. *J Biomed Mater Res*, Vol. 46, No. 3, pp. 399-407.
- [86] Quarles LD, Yohay DA, Lever LW, Caton R, Wenstrup RJ. (1992). Distinct proliferative and differentiated stages of murine MC3T3-E1 cells in culture: an in vitro model of osteoblast development. *J Bone Miner Res*, Vol. 7, No. 6, pp. 683-692.
- [87] Queally JM, Devitt BM, Butler JS, Malizia AP, Murray D, Doran PP, O'Bryne JM. (2009). Cobalt ions induce chemokine secretion in primary human osteoblasts. *J Orthop Res*, Vol. 27, No. 7, pp. 855-864.
- [88] Ragab AA, Van De Motter R, Lavish SA, Goldberg VM, Ninomiya JT, Carlin CR, Greenfield EM. (1999). Measurement and removal of adherent endotoxin from titanium particles and implant surfaces. *J Orthop Res*, Vol. 17, No. 6, pp. 803-809.
- [89] Ramachandran R, Goodman SB, Smith RL. (2006). The effects of titanium and polymethylmethacrylate particles on osteoblast phenotypic stability. *J Biomed Mater Res A*, Vol. 77, No. 3, pp. 512-517.
- [90] Ren PG, Huang Z, Ma T, Biswal S, Smith RL, Goodman SB. (2010). Surveillance of systemic trafficking of macrophages induced by UHMWPE particles in nude mice by noninvasive imaging. *J Biomed Mater Res A*, Vol. 94, No. 3, pp. 706-711.
- [91] Ren PG, Irani A, Huang Z, Ma T, Biswal S, Goodman SB. (2011). Continuous infusion of UHMWPE particles induces increased bone macrophages and osteolysis. *Clin Orthop Relat Res*, Vol. 469, No. 1, pp. 113-122.

- [92] Ren PG, Lee SW, Biswal S, Goodman SB. (2008). Systemic trafficking of macrophages induced by bone cement particles in nude mice. *Biomaterials*, Vol. 29, No. 36, pp. 4760-4765.
- [93] Rodrigo AM, Martinez ME, Escudero ML, Ruiz J, Martinez P, Saldana L, Gomez-Garcia L, Fernandez L, Cordero J, Munuera L. (2001). Influence of particle size in the effect of polyethylene on human osteoblastic cells. *Biomaterials*, Vol. 22, No. 8, pp. 755-762.
- [94] Rodrigo AM, Martinez ME, Saldana L, Valles G, Martinez P, Gonzales-Carrasco JL, Cordero J, Munuera L. (2002). Effects of polyethylene and alpha-alumina particles on IL-6 expression and secretion in primary cultures of human osteoblastic cells. *Biomaterials*, Vol. 23, No. 3, pp. 901-908.
- [95] Roebuck KA, Vermes C, Carpenter LR, Fritz EA, Narayanan R, Glant TT. Down-regulation of procollagen  $\alpha 1$ [I] messenger RNA by titanium particles correlates with nuclear factor  $\kappa$ B (NF- $\kappa$ B) activation and increased Rel A and NF- $\kappa$ B1 binding to collagen promoter. (2001). *J Bone Miner Res*, Vol. 16, No. 3, pp. 501-510.
- [96] Sabokbar A, Fujikawa Y, Brett J, Murray DW, Athanasou NA. (1996). Increased osteoclastic differentiation by PMMA particle-associated macrophages. *Acta Orthop Scand*, Vol. 67, No. 6, pp. 593-598.
- [97] Sabokbar A, Fujikawa Y, Murray DW, Athanasou NA. (1997). Radio-opaque agents in bone cement increase bone resorption. *J Bone Joint Surg Br*, Vol. 79, No. 1, pp. 129-134.
- [98] Sabokbar A, Fujikawa Y, Murray DW, Athanasou NA. (1998). Bisphosphonates in bone cement inhibit PMMA particle induced bone resorption. *Ann Rheum Dis*, Vol. 57, No. 10, pp. 614-618.
- [99] Schofer MD, Fuchs-Winkelmann S, Kessler-Thones A, Rudisile MM, Wack C, Paletta JR, Boudriot U. (2008). The role of mesenchymal stem cells in the pathogenesis of Co-Cr-Mo particle induced aseptic loosening: an in vitro study. *Biomed Mater Eng*, Vol. 18, No. 6, pp. 395-403.
- [100] Seo SW, Lee D, Cho SK, Kim AD, Minematsu H, Celil Aydemir AB, Geller JA, Macaulay W, Yang J, Young-In Lee F. (2007). ERK signaling regulates macrophages colony-stimulating factor expression by titanium particles in MC3T3-E1 murine calvarial preosteoblastic cells. *Ann N Y Acad Sci*, Vol. 1117, pp. 151-158.
- [101] Shida J, Trindade MC, Goodman SB, Schurman DJ, Smith RL. (2000). Induction of interleukin-6 release in human osteoblast-like cells exposed to titanium particles in vitro. *Calcif Tissue Int*, Vol. 67, No. 2, pp. 151-155.
- [102] Sommer B, Felix R, Sprecher C, Leunig M, Ganz R, Hofstetter W. (2005). Wear particles and surface topographies are modulators of osteoclastogenesis in vitro. *J Biomed Mater Res A*, Vol. 72, No. 1, pp. 67-76.
- [103] Takei H, Pioletti DP, Kwon SY, Sung KL. (2000). Combined effect of titanium particles and TNF-alpha on the production of IL-6 by osteoblast-like cells. *J Biomed Mater Res*, Vol. 52, No. 2, pp. 382-387.
- [104] Torii Y, Hitomi K, Tsukagoshi N. (1996). Synergistic effect of BMP-2 and ascorbate on the phenotypic expression of osteoblastic MC3T3-E1 cells. *Mol Cell Biochem*, Vol. 165, No. 1, pp. 25-29.
- [105] Tuan RS, Lee FY, Konttinen Y, Wilkinson JM, Smith RL, Implant Wear Symposium 2007 Biologic Work Group. (2008). What are the local and systemic biologic

- reactions and mediators to wear debris, and what host factors determine or modulate the biologic response to wear particles? *J Am Acad Orthop Surg*, Vol. 16, Suppl 1, pp. S42-48.
- [106] Valles G, Gonzales-Melendi P, Saldana L, Rodriguez M, Munuera L, Vilaboa N. (2008). Rutile and titanium particles differentially affect the production of osteoblastic local factors. *J Biomed Mater Res A*, Vol. 84, No. 2, pp. 324-336.
- [107] Vermes C, Chandrasekaran R, Jacobs JJ, Galante JO, Roebuck KA, Glant TT. (2001). The effects of particulate wear debris, cytokines, and growth factors on the functions of MG-63 osteoblasts. *J Bone Joint Surg Am*, Vol. 83, No. 2, pp. 201-211.
- [108] Vermes C, Roebuck KA, Chandrasekaran R, Dobai JG, Glante TT. (2000). Particulate wear debris activates protein tyrosine kinases and nuclear factor kappaB, which down-regulates type I collagen synthesis in human osteoblasts. *J Bone Miner Res*, Vol. 15, No. 9, pp. 1756-1765.
- [109] Visentin M, Stea S, Squarzoni S, Antonietti B, Reggiani M, Toni A. (2004). A new method for isolation of polyethylene wear debris from tissue and synovial fluid. *Biomaterials*, Vol. 25, No. 24, pp. 5531-5537.
- [110] Wang D, Christensen K, Chawla K, Ziao G, Krebsbach PH, Franceschi RT. (1999). Isolation and characterization of MC3T3-E1 preosteoblast subclones with distinct in vitro and in vivo differentiation/mineralization potential. *J Bone Miner Res*, Vol. 14, No. 6, pp. 893-903.
- [111] Wang ML, Nesti LJ, Tuli R, Lazatin J, Danielson KG, Sharkey PF, Tuan RS. (2002). Titanium particles suppress expression of osteoblastic phenotype in human mesenchymal stem cells. *J Orthop Res*, Vol. 20, No. 6, pp. 1175-1184.
- [112] Wang ML, Tuli R, Manner PA, Sharkey PF, Hall DJ, Tuan RS. (2003). Direct and indirect induction of apoptosis in human mesenchymal stem cells in response to titanium particles. *J Orthop Res*, Vol. 21, No., 4, pp. 697-707.
- [113] Warne BA, Epstein NJ, Trindade MC, Miyanishi K, Ma T, Saket RR, Regular D, Goodman SB, Smith RL. (2004). Proinflammatory mediator expression in a novel murine model of titanium particle-induced intramedullary inflammation. *J Biomed Mater Res B Appl Biomater*, Vol. 71, No. 2, pp. 360-366.
- [114] Wirth MA, Agrawal CM, Mabrey JD, Dean DD, Blanchard CR, Miller MA, Rockwood CA Jr. (1999). Isolation and characterization of polyethylene wear debris associated with osteolysis following total shoulder arthroplasty. *J Bone Joint Surg Am*, Vol. 81, No. 1, pp. 29-37.
- [115] Wolfarth DL, Han DW, Bushar G, Parks NL. (1997). Separation and characterization of polyethylene wear debris from synovial fluid and tissue samples of revised knee replacements. *J Biomed Mater Res*, Vol. 34, No. 1, pp. 57-61.
- [116] Wright T, Goodman SB. (2001). *Implant Wear in Total Joint Replacement*, American Academy of Orthopaedic Surgeons, ISBN 0-89203-261-8, Illinois, United States of America.
- [117] Xiao G, Cui Y, Ducy P, Karsenty G, Franceschi RT. (1997). Ascorbic acid-dependent activation of the osteocalcin promoter in MC3T3-E1 preosteoblasts: requirement for collagen matrix synthesis and the presence of an intact OSE2 sequence. *Mol Endocrinol*, Vol. 11, No. 8, pp. 1103-1113.
- [118] Xiao G, Gopalakrishnan R, Jiang D, Reith E, Benson MD, Franceschi RT. (2002). Bone morphogenetic proteins, extracellular matrix, and mitogen-activated protein

- kinase signalling pathways are required for osteoblast-specific gene expression and differentiation in MC3T3-E1 cells. *J Bone Miner Res*, Vol. 17, No. 1, pp. 101-110.
- [119] Yamanaka Y, Abu-Amer W, Foglia D, Otero J, Clohisy JC, Abu-Amer Y. (2008). NFAT2 is an essential mediator of orthopedic particle-induced osteoclastogenesis. *J Orthop Res*, Vol. 26, No. 12, pp.1577-1584.
- [120] Yamanaka Y, Abu-Amer Y, Faccio R, Clohisy JC. (2006). Map kinase c-JUN N-terminal kinase mediates PMMA induction of osteoclasts. *J Orthop Res*, Vol. 24, No. 7, pp. 1349-1357.
- [121] Yao J, CS-Szabo G, Jacobs JJ, Kuettner KE, Glant TT. (1997). Suppression of osteoblast function by titanium particles. *J Bone Joint Surg Am*, Vol. 79, No. 1, pp. 107-112.
- [122] Zambonin G, Colucci S, Cantatore F, Grano M. (1998). Response of human osteoblasts to polymethylmethacrylate in vitro. *Calcif Tissue Int*, Vol. 62, No. 4, pp. 362-365.
- [123] Zhang H, Ricciardi BF, Yang X, Shi Y, Camacho NP, Bostrom MG. (2008). Polymethylmethacrylate particles stimulate bone resorption of mature osteoclasts in vitro. *Acta Orthop*, Vol. 79, No. 2, pp. 281-288.
- [124] Zilber S, Epstein N, Lee S, Larsen M, Ma T, Smith RL, Biswal S, Goodman SB. (2008). Mouse femoral intramedullary injection model: technique and microCT scan validation. *J Biomed Mater Res B Appl Biomater*, Vol. 84, No. 1, pp. 286-290.
- [125] Zreigat H, Crotti TN, Howlett CR, Capone M, Markovic B, Haynes DR. (2003). Prosthetic particles modify the expression of bone-related proteins by human osteoblastic cells in vitro. *Biomaterials*, Vol. 24, No. 2, pp. 337-346.

IntechOpen



## **Osteogenesis**

Edited by Prof. Yunfeng Lin

ISBN 978-953-51-0030-0

Hard cover, 296 pages

**Publisher** InTech

**Published online** 10, February, 2012

**Published in print edition** February, 2012

This book provides an in-depth overview of current knowledge about Osteogenesis, including molecular mechanisms, transcriptional regulators, scaffolds, cell biology, mechanical stimuli, vascularization and osteogenesis related diseases. Hopefully, the publication of this book will help researchers in this field to decide where to focus their future efforts, and provide an overview for surgeons and clinicians who wish to be directed in the developments related to this fascinating subject.

### **How to reference**

In order to correctly reference this scholarly work, feel free to copy and paste the following:

Richard Chiu and Stuart B. Goodman (2012). Biological Response of Osteoblasts and Osteoprogenitors to Orthopaedic Wear Debris, *Osteogenesis*, Prof. Yunfeng Lin (Ed.), ISBN: 978-953-51-0030-0, InTech, Available from: <http://www.intechopen.com/books/osteogenesis/biological-response-of-osteoblasts-and-osteoprogenitors-to-orthopaedic-wear-debris>

**INTECH**  
open science | open minds

### **InTech Europe**

University Campus STeP Ri  
Slavka Krautzeka 83/A  
51000 Rijeka, Croatia  
Phone: +385 (51) 770 447  
Fax: +385 (51) 686 166  
[www.intechopen.com](http://www.intechopen.com)

### **InTech China**

Unit 405, Office Block, Hotel Equatorial Shanghai  
No.65, Yan An Road (West), Shanghai, 200040, China  
中国上海市延安西路65号上海国际贵都大饭店办公楼405单元  
Phone: +86-21-62489820  
Fax: +86-21-62489821

© 2012 The Author(s). Licensee IntechOpen. This is an open access article distributed under the terms of the [Creative Commons Attribution 3.0 License](#), which permits unrestricted use, distribution, and reproduction in any medium, provided the original work is properly cited.

IntechOpen

IntechOpen